EFFECTS OF PHOSPHODIESTERASE 4 INHIBITION ON BLEOMYCIN-INDUCED PULMONARY FIBROSIS IN MICE

Inaugural Dissertation
submitted to the
Faculty of Medicine
in partial fulfillment of the requirements
for the PhD-Degree
of the Faculties of Veterinary Medicine and Medicine
of the Justus Liebig University Giessen

by
Udalov, Sergey
of
Omsk, Russia

Giessen, 2009

From the Department of Medicine
Director / Chairman: Prof. Dr. Werner Seeger
of Medicine of the Justus Liebig University Giessen

First Supervisor and Committee Member:	Prof. Dr. Ralph Schermuly
Second Supervisor and Committee Member:	Prof. Dr. Tobias Welte
Committee Member (Chair):	Prof. Dr. Martin Diener
Committee Member:	Prof. Dr. Ralf Middendorff

Date of Doctoral Defense: 12th of October, 2009

I. Table of contents

II. List of figures

III. List of abbreviations

6MWD	6-min walk distance test
AC	adenylate cyclase
AECII	alveolar epithelium type II cell
AECI	alveolar epithelium type I cell
AKAP	A kinase–anchoring protein
AM	alveolar macrophage
AMP	adenosine 5'-monophosphate
ANOVA	analysis of variance
APS	ammonium persulfate
ATP	adenosine 5'-triphosphate
BALF	bronchoalveolar lavage fluid
BLAST	basic local alignment search tool
BSA	bovine serum albumin
cAMP	cyclic adenosine 3'-5'-monophosphate
cGMP	cyclic guanosine 3'-5'-monophosphate
CBP	CREB-binding protein
cDNA	complimentary DNA
CFA	cryptogenic fibrosing alveolitis
CNS	central nervous system
COPD	chronic obstructive pulmonary disease
CREB	cAMP response element binding protein
CRE	cAMP response element
Ct	threshold cycle
D_{Lco}	carbon monoxide diffusing capacity
DNA	deoxyribonucleic acid
dNTP	deoxy-N(adenosine, guanosine, cytidine, thymidine, or uridine) triphosphate
DPLD	diffuse parenchymal lung diseases

DTT	dithiothreitol
ECM	extracellular matrix
EDTA	ethylenediaminetetraacetic acid
EMT	epithelial-to-mesenchymal transition
ERK	extracellular signal-regulated kinase
FDA	Food and Drug Administration
GPCR	G-protein-coupled receptor
Gα	activated Gα subunit of a G-protein
HRP	horseradish peroxidase
IL	interleukin
ILD	interstitial lung diseases
IIP	idiopathic interstitial pneumonias
IPF	idiopathic pulmonary fibrosis
KCl	potassium chloride
KH_2PO_4	potassium di-hydrogen phosphate
LPS	lipopolysaccaride
LR	linker regions
MAPK	mitogen-activated protein kinase
MEK	MAPK/ERK kinase
$MgCl_2$	magnesium chloride
MMP	matrix metalloprotease
MPO	myeloperoxydase
mRNA	messenger RNA
NaCl	sodium chloride
Na_2HPO_4	di-sodium hydrogen phosphate di-hydrate
NCBI	National Center for Biotechnology Information
NE	neutrophil elastase
NF	nuclear factor
NO	nitric oxide
PAGE	polyacrylamide gel electrophoresis
PAI	plasminogen activator inhibitor

PAH	pulmonary arterial hypertension
PASMC	pulmonary artery smooth muscle cell
PBS	phosphate buffered saline
PCR	polymerase chain reaction
PDGF	platelet-derived growth factor
PDE	phosphodiesterase
PF	pulmonary fibrosis
PGE2	prostaglandin E2
PILD	pediatric interstitial lung disease
PKA	protein kinase A
PMSF	phenylmethylsulphonyl fluoride
qPCR	quantitative (real-time) PCR
RNA	ribonucleic acid
ROS	reactive oxygen species
ROX	6-carboxyl-X-rhodamine
RTK	receptor tyrosine kinase
SDS	sodium dodecyl sulfate
SEM	standard error of the mean
TBS	tris buffered saline
TBST	tris buffered saline with tween
TEMED	tetramethylethylenediamine
TF	tissue factor
TGF	transforming growth factor
TLC	total lung capacity
TLR	toll-like receptor
TNF	tumor necrosis factor
Tris	tris(hydroxymethyl)aminomethane
UCR	upstream conserved region
UDG	uracil DNA glycosylase
UIP	usual interstitial pneumonia
WD-HBE	well-differentiated human bronchial epithelium

IV. Summary

Pulmonary fibrosis (PF) is an irreversible and largely untreatable human disease with the causes often remaining unknown. Phosphodiesterase 4 (PDE4) is involved in the processes of inflammation, cell proliferation, differentiation and migration that are known to play an important role in tissue fibrosis. The aim of the study was, therefore, to determine the expression of PDE4 under conditions of PF and to investigate the effects of PDE4 inhibition on functional, histological and biochemical parameters in experimental PF.

Pulmonary fibrosis was induced by cytostatic and profibrotic agent bleomycin in C57BL/6N mice. Expression profiles of the different PDE4 isoforms were analyzed at mRNA and protein levels in lungs with both experimental and human PF. Animals were treated with the selective PDE4 inhibitor cilomilast and/or vehicle and treatment effects were examined by means of bronchoalveolar lavage fluid (BALF) differential cell count, mRNA analysis for lung tumor necrosis factor (TNF)-α, interleukin (IL)-1β, IL6, pulmonary compliance measurement, quantified pathological examination of the lungs, collagen assay and survival analysis.

Analysis of PDE4 expression showed significant upregulation of inflammation-related PDE4 isoform in lungs with both human and experimental PF. Treatment of mice with cilomilast resulted in significant reduction in total number of cells, number of macrophages and lymphocytes, but not neutrophils, in BALF at early inflammatory fibrosis stage (days 4 and 7). Lung TNFα, but not IL1β, level was also significantly reduced by cilomilast while level of IL6 was significantly elevated. At later stage (days 14 and 21) cilomilast-treated mice demonstrated improved lung function and lesser fibrosis degree compared to non-treated group. Lung collagen content and overall survival were also partially restored by treatment with cilomilast.

Our results suggest that selective PDE4 inhibition suppresses early inflammatory stage and has the potential to attenuate the late stage of pulmonary fibrosis in experimental fibrosis and thus may offer a new therapeutic option for patients with PF.

V. Zusammenfassung

Die Lungenfibrose ist eine progressive und meistens tödliche Erkrankung, für die es noch immer keine effektive Behandlung gibt. Die Phosphodiesterase 4 (PDE4) spielt bei verschiedenen zellulären Prozessen wie Entzündung, Proliferation, Differenzierung und Migration eine wichtige Rolle. Das Ziel der vorliegenden Arbeit war die Untersuchung der Rolle der PDE4 in der experimentellen Fibrose. Dazu erfolgten Untersuchungen zur Expression der PDE4 in fibrotischen Lungen und Überprüfung des Effektes einer PDE4-Hemmung auf funktionelle, histologische und biochemische Parameter in einem experimentellen Modell der Fibrose.

Dazu wurde eine Lungenfibrose in C57BL/6N Mäusen durch eine einmalige Gabe von Bleomycin induziert und die Expression der verschiedene PDE4 Isoformen auf mRNA- und Proteinebene bestimmt. Die Versuchstiere wurden weiterhin mit dem selektivem PDE4-Hemmstoff Cilomilast oder mit dem Placebo behandelt. Anschließend wurden die Behandlungseffekte durch Zellzählung der bronchoalveolären Lavage (BAL), Genexpressionsanalyse der Zytokine Tumor-Nekrose-Faktor (TNF) α, Interleukin (IL) 1β, IL6, pulmonale Compliance-Messung, quantifizierte pathologische Lungenuntersuchung, Kollagenanalyse und die Überlebensdauer untersucht. Begleitende Untersuchungen zur Expression der PDE4 Isoformen erfolgten am explantierten Gewebe von Patienten mit Lungenfibrose.

Die Genexpressionsanalyse der PDE4 zeigte eine signifikant erhöhte Expression der entzündungsbedingten Isoformen in Maus- und Humanlunge mit Lungenfibrose. Die Behandlung mit Cilomilast führte zu einer signifikanten Reduktion der totalen Zellnummer, der Nummer von Makrophagen und Lymphozyten, nicht aber der Neutrophilien, in der BAL in der frühen Krankheitsphase (Tage 4 und 7). Der Zytokinspiegel von TNFα wurde signifikant gesenkt, während die Spiegel von IL1β und IL6 unverändert blieben. In der späteren Krankheitsphase (Tage 14 und 24) zeigten die Cilomilast-behandelten Mäuse eine verbesserte Lungenfunktion und weniger Fibrose, im Verglech mit unbehandelte Tieren.

Zusammenfassend kann man sagen, dass im experimentellen Modell der Lungenfibrose eine selektive Hemmung der PDE4 die frühe Entzündungsreaktion unterdrückt und möglicherweise die spätere Krankheitsphase abschwächt. Dies könnte daher eine neue Behandlungsmöglichkeit zur Therapie der Lungenfibrose darstellen.

1. Introduction

1.1. Pulmonary fibrosis

Pulmonary fibrosis represents a number of diseases that involve gradual replacement of the normal lung architecture by connective tissue and mesenchymal cells (scarring). It ultimately affects lung interstitium - the tissue compartment between endothelium of capillaries and epithelium of alveoli. Typical symptoms of PF include shortness of breath, nonproductive (dry) cough and fatigue [1-3].

According to the new classification proposed by American Thoracic Society and European Respiratory Society in 2002 (Fig. 1) pulmonary fibrosis embraces a category of diseases named idiopathic interstitial pneumonias (IIP), which in turn is a part of large group of diffuse parenchymal lung diseases (DPLD), or interstitial lung diseases (ILD). The most common form of PF in IIP category is idiopathic pulmonary fibrosis (IPF) [4].

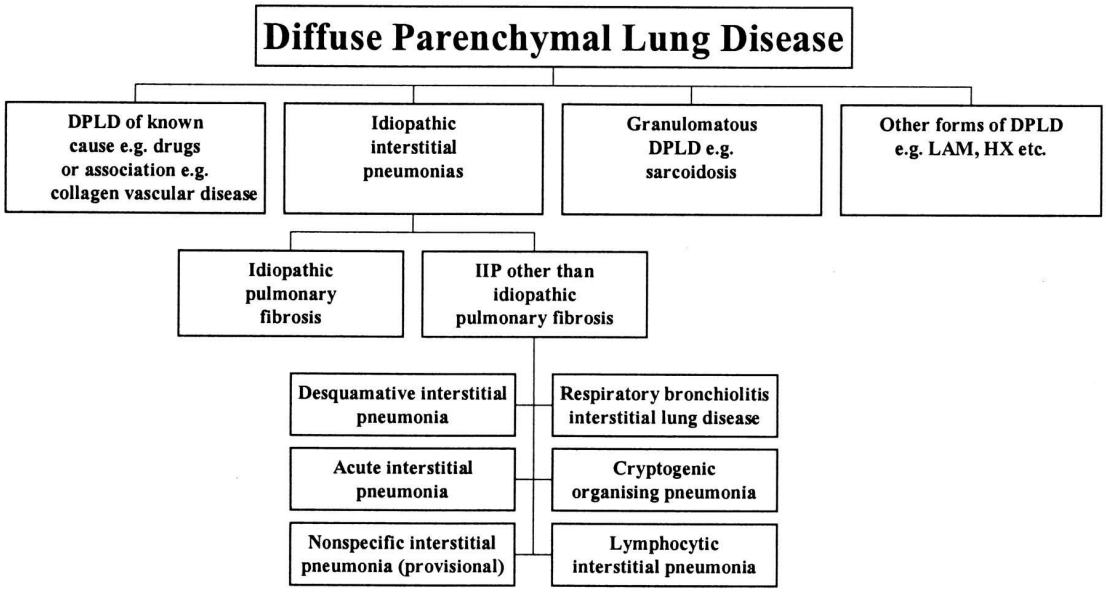

Fig. 1. Current classification of interstitial lung diseases [4]**.**

IPF is a disease of unknown etiology affecting primarily males with prevalence of about 20 per 100,000 individuals [5]. At least 5,000,000 people suffer from this disease worldwide with more than 200,000 cases in the United States alone [1]. In the United States PF mortality rates have been increasing from 1970s to 1990s and have dramatically increased since 1990s [6]. IPF affects individuals of any age, however typically patients are in their forties and fifties when diagnosed [1] and risk rapidly increases with the age [2]. PF, namely pediatric interstitial lung disease (PILD) has also been diagnosed in children of less than one year of age [7]. In most of the cases, etiology of PF remains unknown and by definition, the most common form of PF is idiopathic (unknown cause) pulmonary fibrosis, or IPF [2, 4]. Risk factors for developing PF identified so far include chronic aspiration of asbestos, wood and metal dusts [8], high doses of ionizing irradiation [9] or drug-related toxicity [10].

1.1.1. Characteristics of pulmonary fibrosis

Lung function

PF patients show decline in gas exchange (D_{Lco}) and reduction in total lung volume (TLC) that is reflected in 6-min walk distance (6MWD) test. Pressure-volume graphs (lung compliance) indicate increased air pressure during inflation suggesting stiff non-compliant lung [2-3,11-12].

Bronchoalveolar lavage

Bronchoalveolar lavage fluid (BALF) extracted from PF patents contains higher number of total cells. In particular, elevated levels of granulocytes (neutrophils) and monocytes (activated macrophages) as well as cytokines and growth factors for fibroblasts are observed in the lungs of PF patients. Although less common, number of lymphocytes is also known to be increased [2,12-21].

Pathology

PF patients demonstrate abnormal chest radiograph or computer tomography pattern with ground-glass opacities indicating dense fibrosis areas [3,22]. Biopsy or *post mortem* tissue examination show presence of chronic inflammation. Each ILD has its specific histological appearance, being in case of IPF usual interstitial pneumonia (UIP) [4] with thickened interstitium infiltrated by inflammatory cells. Fibrosis areas are composed of masses of connective tissue, with the collagen being the major component [24], and "fibroblast foci". The latter represent the dense structures with myofibroblasts aligned in parallel and are believed to be the centers of ongoing injury (Fig. 2).

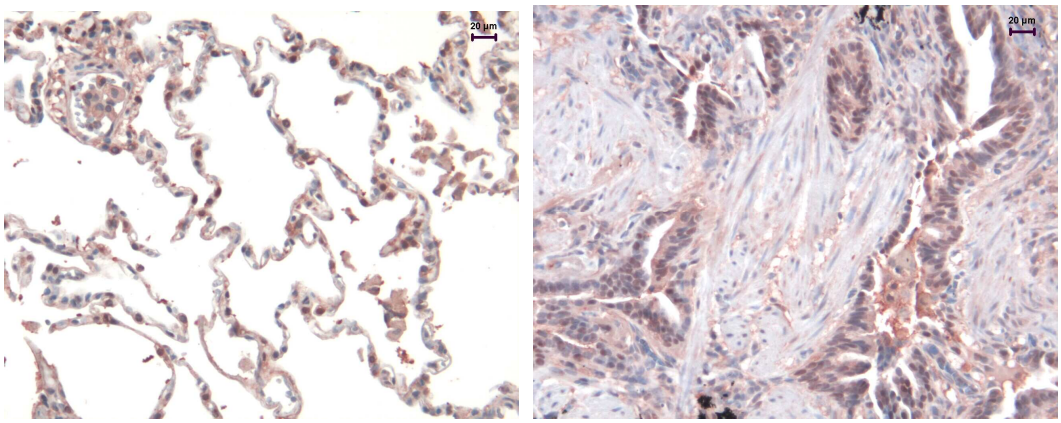

Fig. 2. Histological images of normal (left) and IPF (right) lungs.
Fibroblast focus is present in the center of IPF lung section, magnification x200.

With the time patchy fibrosis is being transformed into massive tissue distortion. So-called "honeycombing" is observed at later PF stages and represents terminal remodeling with non-functional cystically dilated bronchioles containing mucus and inflammatory cells (Fig. 3) [2,22-23]

Inflammation in pulmonary fibrosis

Chronic inflammation is a hallmark of PF and the presence of increased amounts of inflammatory cells both in alveolar space and lung interstitium is well described. Under normal conditions macrophages differentiated from blood monocytes represent the major defense cell population in the lung while granulocytes (neutrophils) and lymphocytes are generally not present. In contrast, number of all inflammatory cells is dramatically increased in BALF of PF patients with boost in the number neutrophils and lymphocytes. In general, an increase in total BALF cell number is mostly accounted for macrophages, however maximal relative increase is accounted for granulocytes and lymphocytes, often reaching 100s-fold. [2,12-13,16-17]

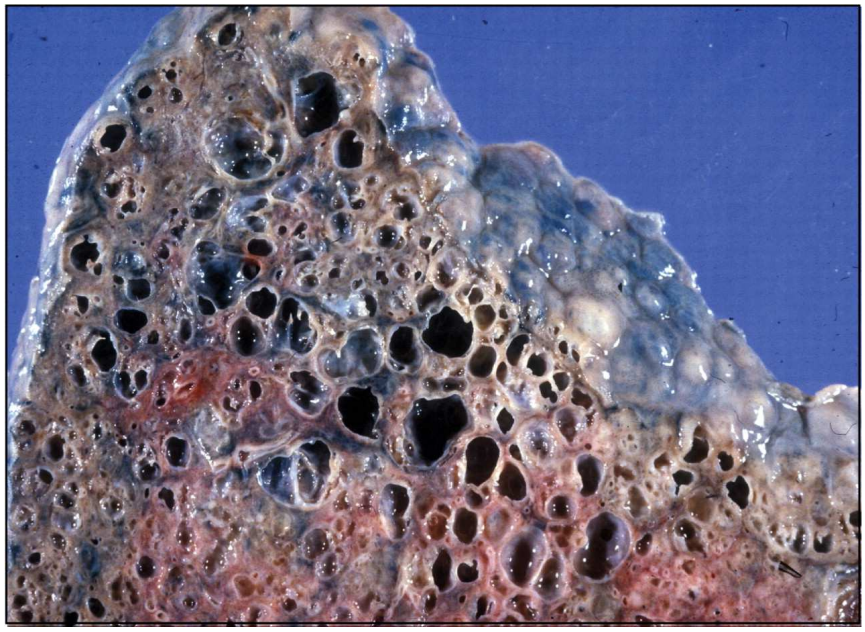

Fig. 3. Lung with end-stage pulmonary fibrosis and honeycombing [3].

Macrophages are believed to play crucial role in tissue fibrosis. Once activated they, together with lymphocytes, secrete cytokines such as TNFα and IL1β

that stimulate proliferation and migration of other cells, such as fibroblasts/myofibroblasts, and, therefore, promote tissue remodeling and fibrosis. Neutrophils play an important role in tissue remodeling as well. They are the potent sources of primary (elastase and myeloperoxydase, MPO) and secondary (collagenase and lactoferrin) granule enzymes, as well as high concentrations of oxidants [12,25]. Thus, in contrast to macrophages, neutrophils themselves may mediate severe tissue remodeling and distortion as it is seen, for instance, in case of COPD [26].

Neutrophil elastase (NE) is released by neutrophils together with other granule enzymes. It is capable of tissue damaging and remodeling through activation of matrix metalloproteases (MMPs). Indeed, PF patients have higher concentrations of proteolytic granule enzymes, such as MPO, collagenase, NE, lactoferrin in BALF [12], as well as increased NE levels in plasma and lung tissue [14]. Interestingly, mice lacking NE are resistant to experimental pulmonary fibrosis [27].

TNFα is a cytokine that is largely secreted by macrophages, although other sources include alveolar epithelium type II cells (AECII) and fibroblasts [15-16,21]. Binding of TNF activates inflammatory response through nuclear factor (NF)-kB pathway and proliferation and differentiation through MAPK-pathway [25]. TNF directly stimulates lung fibroblasts proliferation and production of major lung collagen types, namely 1 and 3 [28-29]. Its protein and mRNA production is elevated in the lungs and BALF of IPF patients [15-16,21]. Moreover, inhibition of TNF by its soluble receptor was alone sufficient to attenuate PF in mice [30].

IL1β is also produced by macrophages [15]. IL1β stimulates expression of adhesion factors on endothelial cells, as well as lymphocyte maturation and proliferation. It also stimulates proliferation of fibroblasts and their production of collagen [28]. Alveolar macrophages (AM) isolated form lungs of IPF, sarcoidosis or asbestos-induced lung disease patients secrete higher levels of this protein [15,18].

IL6 is released primarily by T-cells and macrophages in response to TLR stimulation but can also be secreted by fibroblasts [15,28]. It is presented at significantly higher concentrations in the lungs of IPF patients [15,17,19-20]. However, the role of IL6 in tissue remodeling and inflammation remains controversial: it was shown both to elicit and suppress inflammation [31-32].

Interestingly, the action of the mentioned cytokines also depends on their combination. As such, TNF and IL1 individually stimulate fibroblast proliferation. However, when combined they cause inhibition of proliferation and inhibition of collagen 1 and 3 production. Fibroblasts also start producing IL6 when stimulated by IL1 or TNF and the combination of the two stimulates them even further [28].

1.1.2. Molecular aspects of pulmonary fibrosis

Molecular mechanisms of PF remain unclear. However, some consistent pathological events at cellular and molecular level have been well described (Fig. 4).

In general, lung alveolar epithelium is damaged in PF and this particularly involves the loss of AECI and hyperplasia of AECII [33]. Fibroblasts might be involved in this process since, when isolated from IPF lungs, they were shown to induce epithelial apoptosis *in vitro* [34]. Alveolar damage is accompanied by the presence of pro-coagulatory and pro-inflammatory environment in lungs with PF. For instance, tissue factor (TF) and plasminogen activator inhibitor (PAI)-1 and -2 are strongly expressed by IPF alveolar epithelial cells [35].

On the other hand, fibroblasts isolated from PF lungs show higher rate of proliferation and increased resistance to apoptosis [36]. However, the question of increased survival of IPF fibroblasts is still controversial. For instance, some authors could observe higher apoptosis rate and decreased proliferation rate in IPF fibroblasts [37]. In general, recent hints indicate that RAS/RAF/MEK/ERK pathway (Ras inhibitor, Rho and p-38 MAPK) is involved in PF [38-40].

It was shown in PF that fibroblasts differentiate into myofibroblasts which are characterized by intermediate state between fibroblasts and smooth muscle cells [21,37,41]. Fibroblasts are believed to be attracted by inflammatory cells and AECII through pro-fibrotic mediators, such as TNFα, TGFβ and PDGF, which stimulate their migration and differentiation into myofibroblasts [15-16,28-29]. Indeed, fibroblasts/myofibroblasts isolated from PF lungs demonstrate increased migration capacity [42].

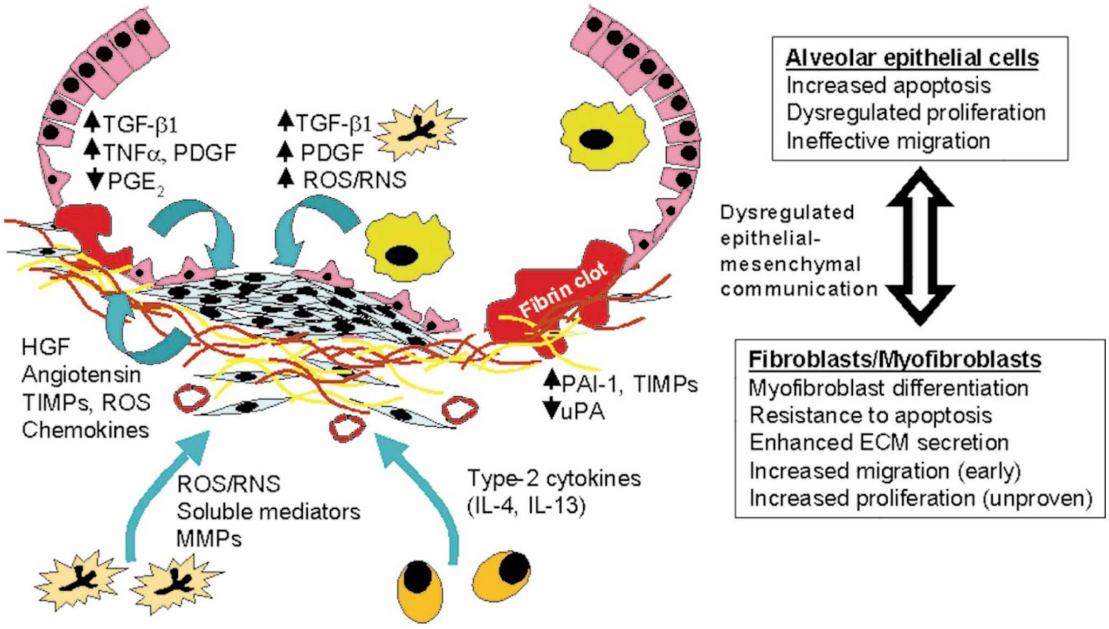

Fig. 4. Dysregulated cell signaling in pulmonary fibrosis [48].

It was long believed that the interstitium is the sole source of myofibroblasts in PF. Recent studies, however, showed that AEC might trans-differentiate into fibroblasts via the process of epithelial-to-mesenchymal transition (EMT) *in vivo* during the course of PF [43-44]. Other cell types, such as circulating fibrocytes, might also serve as a potential source of fibroblasts in PF [45].

Extracellular matrix (ECM) homeostasis is known to be dysregulated in PF. Namely, expression of macrophage- and fibroblast-related MMP1 and -9 is higher in PF [37,46-47]. This imbalance, in turn, is believed to lead to tissue remodeling through facilitated mesenchymal cell migration and basal membrane destruction [23,48]. Another side of ECM homeostasis distortion in PF involves significantly higher lung collagen levels and fibroblasts are believed to be its major source [24,37]. However, some reports show that IPF and normal fibroblasts synthesize similar amounts of collagens [49].

Based on these findings two hypotheses for the development of PF have been proposed so far. The classical “inflammatory” hypothesis states that tissue damage in general, and fibrosis in particular, results from chronic inflammation that is left untreated. Newer so-called “epithelial/mesenchymal” hypothesis states that inflammation itself is not necessary for the development of fibrosis. Instead, internal dysregulation of growth/survival pathways, involving for instance TGFβ, is alone sufficient to cause PF. This hypothesis, however, suggests the presence of some unknown “injury” that triggers the abnormal wound healing process. Therefore, full understanding of the pathological process is still lacking [23,48,50].

1.1.3. Experimental pulmonary fibrosis

Over the past four decades number of agents and techniques have been introduced to generate PF “on demand” in different species (Fig. 5). These approaches, however, can only mimic different aspects of the human disease and none of them represents the true clinical condition [51]. Bleomycin-induced lung fibrosis, introduced in 1970s first in dogs [52] and later in mice [53], represents the most common animal model of PF nowadays [51,54].

Exogenous Agent/Approach	Nature of Tissue Damage	Animal Species Used
Bleomycin	Oxidant-mediated DNA scission leading to fibrogenic cytokine release	Mice, rats, hamsters, rabbits, dogs, primates, pheasants
Inorganic particles (silica, asbestos)	Type IV hypersensitivity reactions with or without granuloma formation	Mice, rats, hamsters, sheep, rabbits
Irradiation	Free radical-mediated DNA damage	Mice, rats, rabbits, dogs, hamsters, sheep, primates
Gene transfer (TGF-β, IL-1β, GM-CSF)	Downstream activation of specific cytokine pathway/s	Mice, rats
Fluorescein isothiocyanate	Incompletely understood. Presumed T-cell-independent.	Mice
Vanadium pentoxide	Incompletely understood. An inorganic metal oxide.	Mice, rats
Haptenic antigens (e.g. trinitrobenzene sulphonic acid compounds)	Recall cell-mediated immune response	Mice, hamsters

Fig. 5. Approaches to inducing experimental pulmonary fibrosis [54].

Bleomycin is an antibiotic isolated from a strain of *Streptomyces verticillus* that is used to treat a variety of cancers [55]. The major limitation of bleomycin therapy is delayed high lung toxicity resulting in PF in about 10% of patients [10]. It is believed that specific toxicity of the drug is accounted for low activity of bleomycin hydrolase in the lung and high concentration of oxygen which is directly related to cytotoxicity [10,56-57].

In mice, PF is typically induced by intra- or orotracheal instillation of bleomycin solution into the lung. The drug produces massive oxidative damage to the tissue followed by acute inflammatory response and, finally, fibrosis. At the molecular level, bleomycin intercalates into DNA groove and forms a complex with ferrous ions and molecular oxygen. Ferrous ions chelated by bleomycin reduce molecular oxygen producing reactive oxygen species (ROS) that cause DNA strand brakes [10,56,58].

First, or “early”, phase of bleomycin-induced fibrosis involves inflammatory response of the lung to oxidative stress and tissue damage. At this stage, lasting as a rule from day 0 till day 7 after the instillation, number of all inflammatory cells in BALF rises dramatically. Similarly to human PF, this increase involves burst (100s-fold increase) in the number of neutrophils and lymphocytes in BALF of the animals [59-63]. At the early stage lung levels of pro-inflammatory cytokines typical for human PF are elevated as well. A such, mice with bleomycin-induced PF express higher amounts of IL1β, TNFα, IL6 and somewhat TGFβ with maximum at around 4 and 7 days being therefore canonical early inflammatory markers [39,60,64].

Later fibrosis stage develops after days 7-10 when lung collagen levels, reflected in lung hydroxyproline content, start to elevate indicating active tissue remodeling [17,59]. MMPs, including MMP9 [39] and other pro-fibrotic markers, such TGFβ1, fibronectin, procollagen-1 also become upregulated [62].

It is believed that experimental PF is fully established in mice at day 21 after bleomycin instillation. At this time typical fibrosis characteristics similar to those, observed in human lungs are present. Namely, lung compliance is dramatically decreased, lung pathology shows significant degree of fibrosis and lung collagen levels are elevated. However, Izbicki et al. and the author of the present work suggest

that established PF can be observed as early as day 14 after bleomycin instillation [65].

Bleomycin-induced pulmonary fibrosis, however, is not able to fully reproduce the real pathological condition in humans. The limitations, besides its inflammatory nature and rapid progression, include the absence of the true fibroblast foci and its partial self-resolution [51,65]. It is also interesting that in contrast to human PF bleomycin-induced fibrosis is female-prevalent [66]. Overall however, BALF cell composition, cytokine profiles, cell behavior and ECM changes during fibrosis process well resemble human PF, in particular in the absence of an ideal model.

1.1.4. Prognosis and treatment

Pulmonary fibrosis in general and IPF in particular is largely an irreversible disease. At least 45,000 individuals die of IPF each year that is more than of breast cancer [1]. Mean survival usually ranges between 2 and 4 years [67], although individual profiles may vary significantly. The latest study indicates that accelerated variant of IPF can progress to death in less than 6 months [69]. Majority of patients die of respiratory insufficiency (38.7%). Other causes of death include heart failure (14.4%), bronchogenic carcinoma (10.4%), ischemic heart disease (9.5%) and infection (6.5%) [68]. It was also reported that PF greatly increases risk of lung cancer [70], although this association is still controversial [71].

Conventional management of PF is based on the concepts of ongoing inflammation on the one hand and fibroblast proliferation/collagen production on the other hand. Therefore, it includes anti-inflammatory (corticosteroids, e.g. prednisolone) and anti-proliferative (cytotoxic, e.g. azathioprine, cyclophosphamide) components [3]. Despite its wide use proof of the effectiveness of this therapy has been lacking. Recent study confirmed that colchicine, cyclophosphamide and prednisone alone or in combination were not able to affect even the course of

moderate IPF [72]. At the same time, such therapy involves serious side effects, including osteoporosis and suppression of immune system [73].

New therapeutic approaches involve more specific interventions, such as inhibition of collagen production by pirfenidone [74] and fibroblast migration/proliferation by interferon and tyrosine kinase inhibitor imatinib (Gleevec™) [63,75]. Restoration of lung level of anti-oxidant glutathione by N-acetylcysteine was also suggested to be promising to prevent lung tissue damage [76]. More sophisticated approaches, such as use of monoclonal antibodies [77], administration of anti-sense oligonucleotides [78], transplantation of living AECII [79] or stem cells [80-81] were also proposed to have beneficial effect on PF in an animal model.

However, the approaches mentioned above were not able to bring significant change in management of PF so far as they are either ineffective or are too far from application in clinic [2-3,22]. Therefore, another approach might involve use of proven and safe therapeutic compounds. Such translational approach can be illustrated by the example of use of the PDE5 inhibitor sildenafil for therapy of ventilation/perfusion mismatch in IPF complicated with secondary PAH [82]

Presently, lung transplantation is the only effective treatment of PF. This disease is the second (26%) leading indication for single lung transplantation after COPD/Emphysema. However, even this radical measure is generally not able to prolong the patient's survival for more than 10 years [83]. New therapeutic approaches are therefore necessary for improved management of PF.

1.2. Phosphodiesterases

Phosphodiesterases (PDEs) are a superfamily of enzymes that selectively catalyze the hydrolysis of the 3'-cyclic phosphate bonds of cAMP and/or cGMP (Fig.6). These are also referred to as class I of phosphodiesterases, in contrast to a broader class II, which members are specific for phosphodiester bond hydrolysis in general [84].

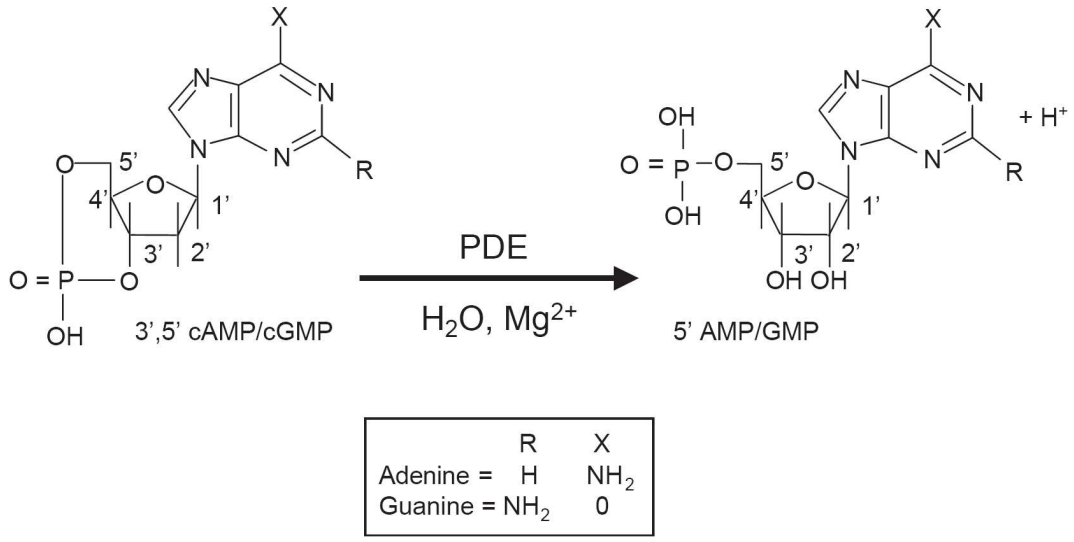

Fig. 6. Hydrolysis of cyclic nucleotides by phosphodiesterases [86].

As second messengers, cAMP and cGMP play an important role in amplifying and spreading the signal from receptors down to the cell interiors. The intensity and duration of their action, however, must be tightly regulated. Therefore, PDEs play the major role in controlling the second messengers' levels in the cell [25].

PDEs are the conservative enzymes that are present in very early spices, for instance in bacteria, fungi and yeasts. Primitive metazoa, such as *Caenorhabditis elegans* and *Drosophila* express quite broad spectrum of PDEs [85].

There are 21 PDE genes identified so far in human, mouse and rat since 1962 when cAMP-phosphodiesterase activity was first described. They are grouped into 11 families based on structural similarity, enzymatic properties and sensitivity to endogenous regulators and inhibitors. Some PDEs selectively recognize and hydrolyze cAMP (PDEs 4, 7, and 8), some selectively hydrolyze cGMP (PDEs 5, 6, and 9), and some can hydrolyze both substrates (PDEs 1, 2, 3, 10, and 11) [84,86-87]. Redundant amount of enzymes for hydrolysis of the same substrate represents the perfect regulation system since different enzymes are regulated through different mechanisms. Thereby it gives the opportunity to different cell components to have access to regulation of the second messenger level. As a rule, PDE family consists of several genes (eg. PDE4 A, B, C and D) each of which might generate multiple products by alternative splicing. Thus, there are at least tens of different products within the whole PDE superfamily [87].

1.2.1. PDE4 overview

The PDE4 family (E.C. 3.1.4.17) belongs to the cAMP-specific PDEs and being the phosphoric diester hydrolases they catalyze the reaction [88]:

adenosine 3'-5'-cyclic monophosphate + H_2O <=> adenosine 5'-monophosphate

PDE4 family represents the largest PDE family, consisting of 4 genes (PDE4A, PDE4B, PDE4C, and PDE4D) with various alternative mRNA splice variants resulting in more than 20 different PDE4 proteins [87,89].

1.2.2. PDE4 protein structure

PDE4s generally consist of conserved catalytic domain and regulatory N- and C-termini (Fig. 7). N-terminus is extremely important in terms of regulation and contains membrane-anchoring domain, linker regions (LR) and upstream conserved regions (UCRs), UCR1 and UCR2. UCR1 contains protein kinase A (PKA)

phosphorylation site (serine). UCR1 and UCR2 are also involved in PDE4 dimerization [90]. C-terminus is also involved in regulation and contains ERK phosphorylation site [85].

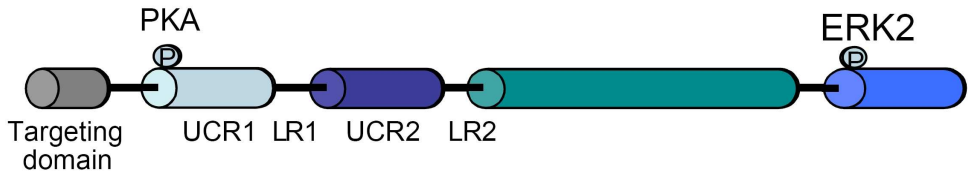

Fig. 7. Functional structure of PDE4 family proteins [86].

All four genes of PDE4 family are categorized into three N-terminal variant groups (“long form,” “short form,” and “super-short form”12) based on the presence or absence of N-terminal UCR domains. Long PDE4 isozymes exhibit both UCR1 and UCR2, whereas short and super-short PDEs lack UCR1 [87]. Short and super-short PDE4s due to lack of UCR1 are not activated by PKA and are monomeric [90].

The catalytic domain of PDE4 consisting of 270 amino acids is composed of alpha helices that form a pocket where the substrate or inhibitors bind. Zn2+ and Mg2+ are necessary for the catalysis and are present in the catalytic center. Hydrogen bonds of multiple helices are thought to orient the purine base, the ribose, and the cyclic phosphate in the catalytic-binding pocket. In spite of the wealth of information on the structure of the catalytic domain, no structure for any PDE holoenzyme has been presented to date. Thus, little is known about the relationship between the catalytic and N- and C-termini of the protein [85,91].

1.2.3. PDE4 expression pattern

PDE4 with all its isoforms is ubiquitously expressed and is also represented in the lung [92-96], including fibroblasts [97-98] and bronchial epithelium cells [99].

Besides the lung, PDE4 is the main cAMP-hydrolyzing enzyme in monocytes, lymphocytes and neutrophils and PDE4B represents the major PDE4 gene expressed in the inflammatory cells [95,100-102]. Expression of PDE4, in particular PDE4D, is also prominent in the brain tissue [92-94,96].

1.2.4. PDE4 function

PDE4 modulates the amplitude and duration of the β-receptor signal and therefore regulates such critical cellular processes as proliferation, differentiation and migration. Specifically, it is a component of cAMP signaling pathway starting at G-protein-coupled receptors (GPCR) linked to G_s proteins (i.e. β-adrenoreceptors). Their activation, for instance, by adrenaline, glucagone or prostaglandins, causes activation of adenylate cyclase (AC) by G_s α-subunit and production of cAMP. The main effector of cAMP is protein kinase A (PKA), which activates the transcription factor CREB that together with CREB-binding protein (CBP) launches the transcription of target genes whose promoters contain CRE [25]. CREB was found to regulate about 4000 human genes, mainly responsible for metabolism as well as for cell proliferation [103].

Cyclic AMP is deeply involved in inflammatory reactions and in general serves as a suppressor of inflammatory response, for instance by inhibition of the TLR signaling pathway. As such, activation of monocytes by LPS and production of TNFα is accompanied by cAMP downregulation [104-105].

cAMP is also involved in regulation of cell proliferation and appears to be its negative regulator in the lung. It was shown that prostaglandins inhibit lung fibroblast migration, proliferation, and collagen synthesis [106-108,139], as well as differentiation into myofibroblasts [109-110]. cAMP pathway is also integrated with RAS/RAF/MEK/ERK pathway as PKA can directly inhibit c-Raf, although details of this interaction are not fully understood [111].

Obviously, cellular cAMP levels must be tightly controlled and regulated. Therefore cAMP specific PDEs in general, and PDE4 in particular, play crucial role in regulation of cell function. PDE4 is induced after β-adrenergic receptor stimulation via negative feedback loop to bring raised cAMP level down, namely by PKA-mediated phosphorylation of UCR1 domain (Fig. 7) [112-113]. Due to lack of UCR1 short and super-short forms of PDE4 cannot be activated by PKA [90]. Some of PDE4s are membrane-bound and function in macromolecular complexes together with PKA in proximity to the receptors therefore controlling cAMP signaling within specific cell compartment [85,114]. These interactions are mediated by A kinase–anchoring proteins (AKAPs) serving as signaling scaffolds [115-116]. Within a longer time frame, PKA activation causes phosphorylation of CREB, which turns on transcription of PDE4 genes [117].

In addition, activity of PDE4 is regulated by ERK as C-termini of PDE4B, C, and D contain motifs for ERK phosphorylation (Fig. 7). In contrast to PKA, phosphorylation by ERK leads to an inhibition of activity. Therefore, physiologically, it is thought that activation of the MAPK pathway will initially lead to local increases in cAMP. This increase in turn will activate PDE4 phosphorylation by PKA that will cause a return of cAMP to a lower level. Therefore, these two phosphorylation steps probably form a timing loop for controlling the duration of the cAMP signal [116].

Given that cAMP is essential for developing inflammatory response and that PDE4B is the main cAMP hydrolyzing enzyme in immunocompetent cells [95,100-102] PDE4 plays critical role in inflammatory cell function by removing the normal block of cAMP on the inflammatory response. Indeed, PDE4B is required for TNFα production by peripheral blood leukocytes and lung macrophages in response to LPS challenge [104-105,118] as well as for T cell activation and proliferation [119-120]. PDE4B null mice showed dramatic decrease in LPS-stimulated TNF production and were resistant to LPS-induced shock [104-105]; PDE4B along with PDE4D are also required for neutrophil recruitment and chemotaxis which was decreased in in PDE4D-/- and PDE4B-/- mice after LPS inhalation [121]

1.2.5. PDE4 inhibitors and clinical applications

Xanthine derivatives such as caffeine and theophylline were the first known nonselective inhibitors of PDE activity [122]. Although first selective PDE4 inhibitor rolipram (ZK 62711, Schering AG) was proposed in 1970s as an antidepressant compound [123] it was later recognized as a potent inhibitor of inflammatory cell influx; its analogues such as piclamilast (RP-73401) were developed for asthma and COPD treatment. However, use of these substances remained limited due to their CNS-mediated emetic effect [119,124-125]. It was demonstrated that emesis results from inhibition of PDE4D [105] that is highly present in the brain [92-93] and is involved in α2A-adrenoceptor signaling [126]

Thus, several second-generation PDE4 inhibitors, such as cilomilast (Ariflo®, GlaxoSmithKline), roflumilast (Daxas®, Altana) and AWD 12-281 (elbion/GlaxoSmithKline) have been developed that have reduced emetic side effects due to increased selectivity for PDE4B rather that PDE4D isoform.

Cilomilast (Ariflo® or SB 207499, GlaxoSmithKline) [127] [c-4-cyano-4-(3-cyclopentyloxy-4-methoxyphenyl)-cis-1-cyclohexanecarboxylic acid], with IC50 of 95nM, is an oral, second-generation, selective PDE4 inhibitor (Fig. 8). In humans it is rapidly absorbed with bioavailability close to 100%. Maximum plasma concentration (C_{max}) is reached after 1.5 hours and is 0.622 μg/ml for a 7 mg dose; 99.6% of cilomilast is highly bound to plasma albumins [128-129]. The drug is metabolized by the action of cytochrome P450 2C8 [130]. The elimination half-life ($t_{1/2}$) ranges between 7 and 8 hours and steady state is rapidly achieved with twice-daily administration. Pharmacokinetic parameters in males and females are similar. Cilomilast is generally well tolerated up to 15 mg twice a day. Most common adverse reactions include nausea and headache and are experienced after administration of more than 20 mg of the drug. Rare effects involve vomiting, and other gastrointestinal adverse events [128].

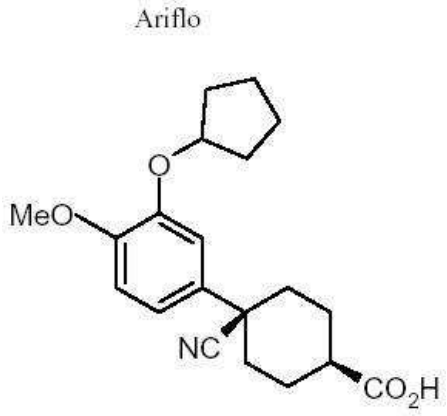

Fig. 8. Chemical structure of cilomilast [131].

In October 2003 the FDA approved Ariflo® for maintenance of lung function in COPD patients poorly responding to salbutamol [131]; other PDE4 inhibitors were proposed for treatment of asthma, arthritis, and psoriasis [84,132].

1.3. PDE4 and fibrosis

The role of PDE4 in tissue fibrosis has not been discussed so far. However, evidences exist that β-adrenoreceptor/adenylate cyclase system together with cAMP/PDE4 might be involved in this pathological process [133].

cAMP is a negative regulator of inflammation [104-105,118,120] which was postulated to be an important component of PF [2,12-20]. PDE4, in turn, is the main cAMP hydrolyzing enzyme in inflammatory cells [95,100-102]. Therefore, elevation of cAMP levels through PDE4 inhibition might potentially attenuate inflammatory side of PF thereby attenuating overall pro-fibrotic environment as well.

Indeed, PDE4 inhibitors, such as rolipram, piclamilast or cilomilast, were shown to suppress TNFα release upon LPS stimulation both *in vitro* [101] and *in vivo* [134-135], including TNFα production in the whole blood from patients with COPD [137]. They were also are able to suppress T-cell activation, proliferation [119-120] and infiltration of inflammatory cells, including neutrophils [136]. Finally, piclamilast and rolipram were demonstrated to inhibit the release of pro-fibrotic cytokine TGFβ both in BALF and tissue in mouse and rat [135,138].

PF is also characterized by abnormal fibroblast behavior expressed in increased proliferation, collagen production and differentiation into myofibroblasts [24,36-37,41-42], as well as by abnormal MMP function [37,46-47]. In turn, elevation of cAMP by PDE4 inhibitors, PGE2 or AC stimulation inhibits lung fibroblast migration, proliferation, and collagen synthesis [106-108,139], as well as their differentiation into myofibroblasts [109-110]. It is also interesting, that fibroblasts from IPF patients have a diminished capacity to generate PGE2 [140]. Similarly, cAMP inhibits proliferation of heart fibroblasts [141] and pulmonary artery smooth muscle cells (PASMCs) [142]. Furthermore, inhibition of PDE4 by cilomilast suppresses release and activation of MMP1, MMP2 and MMP9 from human lung fibroblasts [98,143]. Therefore, PDE4 inhibitors might immediately affect tissue remodeling. Our group has also previously demonstrated that PDE3/4 inhibitor tolafentrine attenuated enhanced migration of PASMCs derived from vessels of

pulmonary hypertensive rats *in vitro* and reversed pulmonary vascular remodeling *in vivo* [144].

The points mentioned above suggest that PDE4 inhibitors are able to modulate both inflammatory response, typical for early fibrosis stage, and tissue remodeling, typical for late stage fibrosis. This suggestion is further supported by the findings of Videla et al., who demonstrated amelioration of experimental chronic colitis and reduction in both TNFα and TGFβ and collagen content in the tissue after treatment with PDE4 inhibitor rolipram [138].

2. Aim of the study

Pulmonary fibrosis is a largely irreversible disease characterized by severe tissue remodeling and chronic interstitial inflammation. Experimental pulmonary fibrosis allows dissecting inflammatory and remodeling stages of the disease. PDE4 is an enzyme hydrolyzing second messenger cAMP which, in turn, is involved in suppression of both inflammation and cell growth and proliferation. Besides, PDE4 is the major cAMP-degrading enzyme in inflammatory cells and is also represented in the lung.

Existing data indicate that PDE4 inhibitors could be successfully used as anti-inflammatory and, possibly, as anti-remodeling agents. The aim of this study was, therefore, to investigate the effects of selective PDE4 inhibition on different stages of pulmonary fibrosis in an animal model *in vivo* and to evaluate the direct involvement of PDE4 in the pathological process. Accordingly, the research was mainly focused on:

1. studying the PDE4 expression profiles in human and experimental PF in mice
2. employment of experimental murine model for PF
3. analyzing the effects of PDE4 inhibition on inflammatory component of experimental PF at the early disease stage
4. analyzing the effects of PDE4 inhibition on remodeling component of experimental PF at the late disease stage

3. Materials and Methods

3.1. Materials

3.1.1. Equipment

Animals handling

Balance 1.0-3000g RP 3000 (August Sauter, Switzerland); polycarbonate cages (Tecniplast, Italy) and bottles 250 ml (Tecniplast, Italy).

Surgery

Scissors, forceps, clamps (Fine Scientific Instruments, Germany); scalpels (Feather, Japan); syringes 1, 2, 5, 10, 25 ml (B.Braun, Germany); needles 26-20G (0.45-0.9mm) BD Microlance™ 3 (BD Drogheda, Ireland); lamp KL 200 (Schott, Germany).

Histology

Tissue processor TP1050, paraffin-embedding system EG1140H, cooling plate for paraffin-embedding EG1150C (Leica, Germany); microtome RM2165, mounting bath HI1210, mounting heating plate HI1220 (Leica, Germany); glass slides Super Frost® Plus 75 x 25 x 1mm (R. Langenbrinck, Germany), cover glass 60 x 24 (0.13-0.18 mm) (R. Langenbrinck, Germany), oven (Memmert, Germany).

Microscopy

Microscope Q550IW, objective DMLA, camera DC300F, server CTR MIC (Leica, Germany).

Cell count

Neubauer chamber (depth 0.1 mm, 0.0025 mm2; Optik Labor, Germany); Shandon Cytospin-3® centrifuge (Thermo Scientific, UK); Centrifuge Rotanta/TRC (Hettich,

Germany).

Lung compliance measurement

Robertson box (USI Elektronikwerkstatt at Boehringer Ingelheim, Germany).

RNA and protein isolation

Homogenizer Precellys 24 (Bertin Technologies, France); spectrophotometer NanoDrop® ND-1000 (NanoDrop Technologies, USA); microplate reader Infinite M200 (Tecan, Austria); thermomixer Compact (Eppendorf, Germany); water bath TM 130-6 (Haep Labor Consult, Germany).

Polymerase chain reaction

qPCR system Stratagene Mx3000P™ (Stratagene, USA); plate centrifuge Rotina 46 RS (Hettich, Germany).

Western blotting

Electrophoresis chamber (Biometra, Germany), power supply (Biometra, Germany); electrophoresis glasses set Whatman (Biometra, Germany); semi-dry blotting system (Biometra, Germany); shaker; autoradiography cassettes (Curix, Germany); dark room BioDocAnalyze (Biometra, Germany); film processor Curix 60 (Agfa, Germany).

Other equipment

Micropipettes Reference® 0.5-10, 10-100, 100-1000 µl (Eppendorf, Germany); vortex Vortex-Genie® 2 (Scientific Industries, USA); balance 0.01-200g SAC-51 (ScalTech, USA); balance 0.05-110g Mettler AJ100 (Mettler Toledo, Germany); micro centrifuge Biofuge Fresco (Heraeus, Germany); ice maker Icematic F100 Compact (Castelmac SPA, Italy); fridges for +4 ^{O}C (Bosch, Germany), fridge -20 ^{O}C (Bosch, Germany), ultra-low fridge -80 ^{O}C (Sanyo, Japan).

3.1.2. Reagents and materials

Animal diet

Food Global Diet (Harlan Teklad, UK).

Surgery and animal experiments

Disinfectant Braunoderm® (B.Braun, Germany); Ketavet® (ketaminehydrochloride) 100mg/ml (Pharmacia, Germany); Rompun (xylacinehydrochloride) 2% (Bayer, Germany); isofluran (Baxter, Germany); bleomycin 1.7 U/mg (Sigma, Germany); sterile 0.9% sodium chloride isotonic solution (DeltaSelect, Germany); cilomilast (Nycomed, Germany); methyl cellulose (Sigma, Germany); oxygen 99.5% pure (Linde, Germany); liquid nitrogen (AirLiquid, Germany).

Histology and microscopy

Roti®-Histofix (4.5% formaldehyde), acid-free (Roth, Germany); Roti®-Histol, for histology (Roth, Germany); Xylol (isomere) >98% pure, for histology (Roth, Germany); Pertex® (Medite, Germany); Paraplast Plus (paraffin) embedding medium (Sigma, Germany); Hematoxilin Haemalaun nach Mayer, acidic (Waldeck, Germany); Eosin-Y alcoholic (Thermo Scientific, UK); May Gruenwald (Merck, Germany); Giemsa (Sigma, Germany); sodium chloride (Roth, Germany); potassium chloride (Merck, Germany); di-sodium hydrogen phosphate di-hydrate (Merck, Germany); potassium di-hydrogen phosphate (Merck, Germany).

Molecular biology experiments

TRIzol® reagent (Invitrogen, USA); ImProm-II™ Reverse Transcription System (Promega, USA); Platinum® SYBR® Green qPCR SuperMix-UDG mix (Invitrogen, USA); SIRCOL collagen assay (Biocolor Ltd., UK); RIPA lysis buffer (Santa Cruz Biotechnology, USA); Complete, Mini, EDTA-free protease inhibitor cocktail (Roche, Germany); DC protein assay (Bio-Rad Laboratories, USA); Rainbow™ protein molecular weight maker (GE Healthcare, UK); nitrocellulose blotting membrane BioTrace™ NT (Pall Corporation, USA); ECL plus detection reagent (GE

Healthcare, UK); normal films Cronex 5 (Agfa, Belgium), high-sensitive films Amersham Hyperfilm MP (GE Healthcare, UK); acetic acid, min 99% (Sigma, Germany); chloroform, min 99% (Sigma, Germany); ethanol 99.9% (Stockheimer Chemie, Germany); ethanol 96% (Otto Fischhar, Germany); ethanol 70% (SAV LP, Germany); 2-propanol (Fluka, Germany); RNase away (Molecular Bioproducts, USA);

antibodies:

specific primary antibody	**cross reactivity**	**host**	**dilution**	**manufacturer**
anti-β-actin	mouse, human, rat	mouse	1:5000	Abcam, UK
anti-PDE4A	mouse, human, rat	rabbit	1:1000	Abcam, UK
anti-PDE4B	mouse, human, rat	rabbit	1:1500	Fabgennix, UK
anti-PDE4C	mouse, human, rat	rabbit	1:500	Fabgennix, UK
anti-PDE4D	mouse, human, rat	rabbit	1:1000	Fabgennix, UK
specific secondary antibody				
anti-mouse IgG, HRP-conjugated	-	rabbit	1:50000	Sigma, Germany
anti-rabbit IgG, HRP-conjugated	-	goat	1:50000	Pierce Biotech, USA

oligonucleotides (Metabion, Germany):

target genes	**sequences**	**Tm, ^{o}C**	**product size, bp**
mouse PDE4A	5'-TGGTAGAGACGAAGAAAGTGACC-3' (forward) 5'-CTTGTCACACATGGGGCTAAT-3' (reverse)	59	227 (cDNA) 955 (genomic DNA)
human PDE4A	5'-GAGGACAACTGCGACATCTTC-3' (forward) 5'-CGGTCGGAGTAGTTATCTAGCAG-3' (reverse)	59	191 (cDNA) 387 (genomic DNA)
mouse PDE4B	5'-AATTGCTACAAGAGGAACACTGC-3' (forward)	59	243 (cDNA) 1139 (genomic DNA)

	5’-TATCACACATTGGGCTAATCTCC-3’ (reverse)		
human PDE4B	5’-AGGCGTTCTTCTCCTAGACAACT-3’ (forward) 5’-CCACAGAAGCTGTGTGTTTATCA-3’ (reverse)	59	212 (cDNA) 933 (genomic DNA)
mouse PDE4C	5’-ACCTCAGTACCAAGCAGAGACTG-3’ (forward) 5’-AGAGTAGTTGTCCAAGAGCAGGA-3’ (reverse)	59	164 (cDNA) 549 (genomic DNA)
human PDE4C	5’-GTCCAGACTGACCAGGAGGA-3’ (forward) 5’-GGCATGTAGGCTGTTGTGGTAG-3’ (reverse)	59	246 (cDNA) 882 (genomic DNA)
mouse PDE4D	5’-CACAGCTCCAGCCTAACTAATTC-3’ (forward) 5’-ATGGTGTGCATGATAACAGTCAG-3’ (reverse)	59	170 (cDNA) 1365 (genomic DNA)
human PDE4D	5’-ACCGGATAATGGAGGAGTTCTT-3’ (forward) 5’-CTCTGGTACCATTCACGATTGTC-3’ (reverse)	59	223 (cDNA) 799 (genomic DNA)
mouse TNFα	5’-GGCCTCCCTCTCATCAGTTCTAT-3’ (forward) 5’- ACGTGGGCTACAGGCTTGTC-3’ (reverse)	60	86 (cDNA) 254 (genomic DNA)
mouse IL1β	5’-GAGCACCTTCTTTTCCTTCATCT-3’ (forward) 5’-GATATTCTGTCCATTGAGGTGGA-3’ (reverse)	59	196 (cDNA) 739 (genomic DNA)
mouse IL6	5’-TCAATTCCAGAAACCGCTATGAA-3’ (forward) 5’-CACCAGCATCAGTCCCAAGAA-3’ (reverse)	61	78 (cDNA) 243 (genomic DNA)
mouse β-actin	5’-CTCTAGACTTCGAGCAGGAGATG-3’ (forward) 5’-CACTGTGTTGGCATAGAGGTCTT-3’ (reverse)	59	236 (cDNA) 331 (genomic DNA)
human β-actin	5’-TTAAGGAGAAGCTGTGCTACGTC-3’ (forward) 5’-ATGGAGTTGAAGGTAGTTTCGTG-3’ (reverse)	59	211 (cDNA) 306 (genomic DNA)

Other materials

96-well PCR plates ABgene® (Thermo Scientific, UK); 96-well plates Costar® (Coring Inc, USA); sterile PP-Tubes 0.2, 0.5, 1.5, 2.0 ml (SARSTEDT, Germany);

sterile PP-Tubes 15, 50 ml Cellstar® (Greiner Bio-One, Germany); pipette tips 20, 200, 1000 µl epT.I.P.S. standard (Eppendorf, Germany); pipette tips 10, 100, 1000 µl DNase/RNase free (Nerbe Plus, Germany); gloves Nitra-Tex® (Ansell, China) and Nobaglove® latex (NOBA Verbandmittel Danz, Germany).

3.1.3. Software

Animal experiments

Atembox Messung v1.1 (Boehringer Ingelheim, Germany); Leica QWin3 Standard v3.3.1 (Leica Microsystems, Switzerland); Leica QGo Routine Runner v3.2.0 (Leica Microsystems, Switzerland).

Molecular biology experiments

GenBank and BLASTn (National Center for Biotechnology Information, USA); Primer3 v.0.4.0 (Rozen S and Skaletsky HJ, SourceForge); UCSC In-Silico PCR (Jim Kent, University of California Santa Cruz); MxPro™ QPCR software v.3.00 (Stratagene, USA); NanoDrop ND-1000 v3.3.0 (Coleman Technologies, USA); Magellan v.6.3 (Tecan, Austria); i-Control (Tecan, Austria).

Statistics

Prism® v5.01 (GraphPad Software, USA); MS® Excel 2000 (Microsoft, USA).

3.2. Methods

3.2.1. Animals

Adult male 5-6 weeks-old C57BL/6N mice weighting 19-21 g were obtained from Charles River Laboratories (Sulzfeld, Gemany). Animals were housed under room temperature and 12/12-hour light/dark cycle with free access to food and water.

All experiments were performed in accordance with the “National Institutes of Health Guidelines on the Use of Laboratory Animals”. Both the University Animal Care Committee and the Federal Authorities for Animal Research of the Regierungspräsidium Giessen (Giessen, Germany) approved the study protocol.

3.2.2. Human material

Human lung tissue was obtained from three donors and four IPF patients that underwent lung transplantation in Medical University of Vienna (Vienna, Austria) and had a confirmed UIP histological pattern. Pieces of lung tissue were snap-frozen immediately upon lung excision and used for mRNA and protein extraction.

The study protocol for tissue donation was approved by the “Ethik-Kommission am Fachbereich Humanmedizin der Justus-Liebig-Universitaet Giessen” of the University Hospital Giessen (Giessen, Germany) in accordance with national law and with the “Good Clinical Practice/International Conference on Harmonisation” guidelines. Written, informed consent was obtained from each individual patient or the patient's next of kin.

3.2.3. Bleomycin administration

At day 0 mice were given anesthesia with inhalation of isofluran (Baxter, Germany) followed by random orotracheal instillation of bleomycin or sterile saline (0.9% NaCl). The animal was fixed in a vertical position under a binocular. During instillation nose of a mouse was kept pinched so that during inspiration bleomycin or saline solutions were inhaled and distributed throughout the lung. Bleomycin (Sigma, Germany) was dissolved in sterile saline to achieve the dose of 2.8 units/kg mouse body weight.

3.2.4. Treatment groups

Animals were assigned to the following groups 1) “saline”, 2) “bleo+ctrl” and 3) “bleo+cilo”. „Saline” group received instillation of sterile saline at day 0 and was given vehicle alone (2% aqueous methylcellulose solution). Mice in “bleo+ctrl” group received instillation of bleomycin at day 0 and were given vehicle alone. Mice in “bleo+cilo” group received instillation of bleomycin at day 0 and were treated once a day with 50 mg/kg cilomilast (SB207499 or Ariflo, [c-4-cyano-4-(3-cyclopentyloxy-4-methoxyphenyl)-r-l-cyclohexane carboxylic acid]) (Nycomed, Germany), suspended in vehicle. Solutions were given *per os* via gavage needle, all at the same time of a day. Treatment in all groups started at day 0 and lasted till the end of experiment, i.e. for 4, 7, 14 or 24 days.

3.2.5. Protein isolation

Left lung lobes snap-frozen in liquid nitrogen and stored at -80^{O}C were used for protein isolation. Tissues were homogenized in complete RIPA lysis buffer (Santa Cruz Biotechnology, USA) with Precellys 24 homogenizer (Bertin Technologies,

France) at 6000 rpm for 20 sec for three times with 0.5 ml lysis buffer per 0.05 g tissue. Complete *1x lysis buffer* contained:

component	**final concentration**
RIPA buffer *	1x
protease inhibitor cocktail	1x
sodium orthovanadate	1%
PMSF	1%

* 1x RIPA contains: 1x TBS, 1% Nonidet P-40, 0.5% sodium deoxychlorate, 0.1% SDS, 0.004% sodium azide.

After homogenization and 15-minutes lysis time samples were centrifuged at 13000 rpm for 20 min at $4^{O}C$ and supernatant was transferred into a fresh tube. Tissue and protein samples were kept on ice during the whole isolation process.

Protein concentration was determined with DC protein assay (Bio-Rad Laboratories, USA) according to manufacturer's instructions. Briefly, protein solution diluted 1:20-1:40 was mixed with Reagent A' (alkaline copper tartrate) and Reagent B (Folin reagent) in a 96-well microplate. BSA at concentrations of 0.2 – 0.4 – 0.8 – 1.6 mg/ml was used as a standard for calibration curve. After developing of color reaction samples were red at 750 nm with microplate reader Infinite M200 (Tecan, Austria). Final protein concentration was determined with accompanying Magellan™ software. After isolation protein samples were frozen immediately and stored at $-80^{O}C$.

3.2.6. Western blotting

Protein samples were mixed with 5x loading buffer and boiled for 10 min at $100^{O}C$. *Protein loading solutions* had the following composition:

component	final concentration
Tris-chloride pH6.8	75 mM
SDS	2%
glycerol	15%
β-mercaptoethanol	2.5%
bromphenol blue	trace
protein	5 μg/μl

Polyacrylamide gels for sodium dodecyl sulfate polyacrylamide gel electrophoresis (SDS-PAGE) were prepared in a following way. First, 10%-resolving gel solution was poured between the electrophoresis glasses. Water was layered on top of the solution and the solution was left for polymerization for at least 30 min. After the polymerization of the resolving gel water was removed and 6%-stacking gel solution was poured. A comb was inserted and polymerization lasted at least 30 min. *SDS-PAGE gels* had the following composition:

component	final concentration	
	stacking gel	resolving gel
acrylamide	6%	10%
SDS	0.1%	0.1%
APS	0.05%	0.05%
TEMED	0.1%	0.1%
Tris-chloride pH6.8	125 mM	-
Tris-chloride pH8.9	-	375 mM

Protein samples were loaded onto the gel with concentrations of 10-25 μg per lane for housekeeping gene and 50-100 μg per lane for target gene. Rainbow™ Protein molecular weight maker (GE Healthcare, UK) was loaded in parallel. SDS-PAGE was run at 90 V to allow the buffer front enter the resolving gel and at 130 volts until the desired separation degree. Power supply (Biometra, Germany) was stabilized by potential difference. Standard vertical electrophoresis chamber (Biometra, Germany) was filled with *1x running buffer* of the following composition:

component	final concentration
Tris	25 mM
glycin	192 mM
SDS	0.1%

After electrophoresis proteins were transferred onto a nitrocellulose blotting membrane BioTrace™ NT (Pall Corporation, USA). Blotting sandwich was assembled in the following sequence: anode – blotting paper (three layers) – blotting membrane – resolving gel - blotting paper (three layers) – cathode. All components were pre-wetted in *1x blotting buffer*:

component	final concentration
Tris	50 mM
glycin	40 mM
methanol	20%

Transfer was carried out in semi-dry blotting system (Biometra, Germany) at 130 mA for 1.5 hours. Power supply (Biometra, Germany) was stabilized by current. After the transfer membrane was placed on shaker for 1 hour in blocking solution containing 5% powdered milk in TBST buffer. *1x TBST* contained:

component	final concentration
Tris	20 mM
NaCl	150 mM
EDTA	5 mM
tween-20	0.1%

Blocking solution was discarded and primary antibodies, diluted up to specific values in TBST containing 5% powdered milk, were added to the membrane for 1 hour. After incubation membranes were washed on shaker in 1x TBST three times for 10 min. Secondary antibodies conjugated to horseradish peroxidase (HRP) were also diluted in 1x TBST containing 5% powdered milk and added to the membranes for 1 hour.

After incubation, membranes were again washed in 1x TBST three times for 10 min. ECL plus detection reagent (GE Healthcare, UK) was then added and signal was developed according to manufacturer's instructions. Briefly solutions A (buffer) and B (Acridan) were mixed with the ratio 40:1 and added to continuously shaking membrane for 5 min in the dark. The resulting chemiluminescence was detected by autoradiography. Normal Cronex 5 (Agfa, Belgium) or high-sensitive Amersham Hyperfilm MP (GE Healthcare, UK) films and cassettes (Curix, Germany) were used. Exposure time was 1-3 min for housekeeping gene and 2-15 min for target genes. Films were developed automatically in Curix 60 film processor (Agfa, Germany).

Results were analyzed with BioDocAnalyze station (Biometra, Germany). Expression was quantified by densitometry with accompanying BioDocAnalyze 2.1 software by normalizing the values to internal control (β-actin).

3.2.7. RNA isolation

For RNA extraction left lung lobes snap-frozen in liquid nitrogen and stored at -80^{O}C were used. Tissues were homogenized in 0.5 ml of TRIzol® reagent per 0.05 g tissue (Invitrogen, USA) with Precellys 24 homogenizer (Bertin Technologies, France) at 6000 rpm for 20 sec. RNA was isolated by *standard protocol*:

steps and reagents (per 0.05 g tissue)
Addition of 0.1 ml of chloroform, shaking vigorously for 10 min at RT
Centrifugation at 13000 rpm for 30 min at 4^{O}C
Transfer of aqueous phase into fresh tube
Addition of 0.25 ml of isopropanol, incubation for 15 min at RT
Centrifugation at 13000 rpm for 20 min at 4^{O}C
Discarding of supernatant
Washing with 70% ethanol
Centrifugation at 13000 rpm for 20 min at 4^{O}C
Air-drying
Dissolving of RNA in 30 µl of RNase-free water
Incubation at 55^{O}C for 10 min

RNA samples were read at wavelengths of 260 and 280 nm with NanoDrop® ND-1000 spectrophotometer (NanoDrop Technologies, Inc, USA). Concentration was determined by accompanying NanoDrop ND-1000 software based on absorbance at 260 nm and extinction coefficient of 40 using *Beer-Lambert equation*:

$$A = E * b * c$$

where ***A*** is the absorbance, ***E*** is extinction coefficient (liter/mol-cm), ***b*** is the path length (cm) and **c** is the analyte concentration (moles/liter). With *b*=1 cm final equation was:

$$RNA\ concentration\ (ng/\mu l) = A260 * 40$$

Purity of RNA (i.e. admixture of phenol and/or protein) was estimated by the ratio A260/A280: RNA samples with the ratio of 1.7-2.0 were considered of good purity. After isolation RNA was frozen immediately and stored at -80^{O}C.

3.2.8. cDNA synthesis

To generate cDNA reverse transcription was carried out with ImProm-II™ Reverse Transcription System (Promega, USA). The first step of cDNA synthesis involved equalization of input RNA concentration and annealing of oligo(dT)$_{15}$ primers. Namely, 5 µl of the reaction mix contained:

component	**final concentration**
oligo(dT)$_{15}$ primer	0.5 µg
RNA	1 µg

Tubes were placed into the thermal cycler with the following program for annealing: heating at 70^{O}C for 5 min and cooling at 4^{O}C for 5 min. The second step

involved DNA synthesis itself. The following components were added to the mixture to make it up to 20 µl volume:

component	final concentration
ImProm-II™ 5X reaction buffer *	1x
$MgCl_2$	2.5 mM
dNTPs	0.5 mM
recombinant RNasin® ribonuclease inhibitor	20 units
ImProm-II™ reverse transcriptase	1/20 volume

* ImProm-II™ 5X reaction buffer contains: 250 mM Tris-chloride (pH 8.3), 375 mM KCl, 50 mM DTT.

Tubes were placed into the thermal cycler programmed as follows: annealing at $25^{O}C$ for 5 min, extension at $42^{O}C$ for 60 min and inactivation of reverse transcriptase at $70^{O}C$ for 15. After the synthesis cDNA was frozen immediately and stored at $-20^{O}C$.

3.2.9. Real-time polymerase chain reaction

Quantitative real-time PCR analysis (qPCR) was carried out using Platinum® SYBR® Green qPCR SuperMix-UDG mix (Invitrogen, USA). cDNA was diluted four times and reaction mix with the final volume of 25 µl contained the following components:

component	final concentration
Platinum® SYBR® Green qPCR SuperMix-UDG 2X mix *	1x
ROX dye	500 nM
$MgCl_2$	4 mM
primer (forward)	0.2 uM
primer (reverse)	0.2 uM
cDNA	0.2 µg

* Platinum® SYBR® Green qPCR SuperMix-UDG 2X mix contains: Platinum® *Taq* DNA polymerase, SYBR® Green I dye, Tris-chloride, KCl, 6 mM $MgCl_2$, 400 µM dGTP, 400 µM dATP, 400 µM dCTP, 800 µM dUTP, uracil DNA glycosylase (UDG) and stabilizers.

Specific primers used were designed to anneal to adjacent exons in order to discriminate the cDNA and possible genomic DNA products by dissociation curve analysis and agarose gel electrophoresis. Source exon sequences were retrieved from NCBI GenBank and primers were designed with Primer3 software with the following parameters: length of 20-25 nucleotides, melting temperature of 57-63^{O}C and GC-content of 40-60%. Obtained primer sequences were compared to all existing DNA sequences in GenBank database with BLASTn software tool to exclude non-specific annealing. Finally, in-silico (virtual) PCR was performed on genomic DNA and mRNA templates using UCSC In-Silico PCR and Sequence Manipulation Suite v2 tools respectively. Quantitative real-time PCR was carried out in Srtratagene Mx3000P™ qPCR system (Stratagene, USA). The instrument was programmed as follows: denaturation, 95°C for 10 min; 40 cycles with denaturation at 95°C for 30 s, annealing at 59-60°C for 30 s and extension at 72°C for 30 s. Results were analyzed with accompanying MxPro™ qPCR software. Relative expression levels were calculated as ΔCt values by normalizing Ct values of target genes to Ct values of β-actin.

3.2.10. Bronchoalveolar lavage fluid (BALF) cell count

After 4 and 7 days after bleomycin instillation mice were sacrificed by injecting i.p.a lethal dose of ketamin/xylacinehydrochloride. Lungs were flushed 3 times with 0.5 ml ice cold PBS-EDTA (1x PBS, 0.2% EDTA) and for each lung these solutions were pooled. *1x PBS* (pH 7.4) contained:

component	final concentration
NaCl	137 mM
KCl	2.7 mM
Na_2HPO_4	10 mM
KH_2PO_4	2 mM

After centrifugation, cells were re-suspended in 1 ml of ice-cold saline. Total cell count was performed manually using Neubauer chamber (depth 0.1 mm, 0.0025 mm^2; Optik Labor, Germany) and the microscope (Leica, Germany). Briefly, 10 µl of BALF solution were applied onto the chamber and cells in each of four areas were counted. Total cell number (in cells per milliliter) was calculated with the following formula:

$$\text{cells / ml} = \frac{[\text{cells in 4 large squares}] \times 1000\,\mu l}{0.4\,\mu l}$$

For differential cell count cells in constant volume of 0.2 ml of PBS were transferred to a glass slide with Shandon Cytospin-3® centrifuge (Thermo Scientific, UK) at 500 rpm for 5 min after what cells were dried. Slides were stained with *May Gruenwald/Giemsa* using the following protocol:

step	duration, min
May Gruenwald	10 min
washing with distilled water	1 min
Giemsa	5 min
washing with distilled water	5 min

Numbers of macrophages, neutrophils and lymphocytes were determined by manual counting on light microscope (Q550IW; Leica, Germany) among 100 of total cells. These data were then extrapolated to number of cells per milliliter.

3.2.11. Lung compliance measurement

After 14 and 24 days after bleomycin instillation mice were subjected to lung compliance measurement using Robertson box (Boehringer Ingelheim, Germany). Animals were deeply anesthetized with ketamin/xylacinehydrochloride (Bayer, Germany) given i.p. Trachea was canulated, mice were placed in the chamber and connected to the instrument. During the experiment temperature of the chamber was maintained at 40^{O}C. Instrument was calibrated for volume of 0.3 ml and pressure of 3 kPa. Inflation volume and inspiration/expiration frequency was set to 0.3 ml and 20 times/min respectively. Measurement lasted for 5 min and compliance was calculated by accompanying Atembox Messung software as a ratio of volume to pressure. Values were expressed as ml/kPa.

3.2.12. Histological examination

After 14 and 24 days of experiment mice were sacrificed for lung isolation by injecting i.p. a lethal dose of ketamin/xylacinehydrochloride. Left bronchus was ligated, the left lobe was excised and shock-frozen in liquid nitrogen for subsequent RNA isolation and hydroxyproline analysis. Four right lobes were inflated with 4.5% formaldehyde solution through the trachea at constant pressure of 10 cm water column. Fixation was carried out for 24 hours at room temperature. Then lungs were transferred to 1x PBS for next 24 hours at $+4^{O}$C. Lungs were dissected into separate lobes, placed into plastic cassettes and incubated for 24 hours at $+4^{O}$C in PBS. After dehydration in graded alcohol in tissue processor (TP1050; Leica, Germany) lung lobes were separately embedded in paraffin (EG1140H; Leica, Germany), sectioned at 3 µm thickness on microtome (RM2165; Leica, Germany), mounted on glass slides and stained using standard *Hematoxilin-Eosin protocol*. Briefly, slides were incubated at 55^{O}C for 20 min in the oven and then immersed in series into the following solutions:

step	duration, min
Rotihistol	10
Rotihistol	10
Rotihistol	5
ethanol 99.6%	5
ethanol 99.6%	5
ethanol 96%	5
ethanol 70%	5
distilled water	2
Hämalaun nach Mayer, acidic	20
tap water	5
ethanol 96%	1
eosin-Y alcoholic	4
distilled water	rinse
ethanol 96%	2
ethanol 96%	2
ethanol 99.6%	5
isopropanol 99.8%	5
Rotihistol	5
Rotihistol	5
xylol	5

Slides then were covered with Pertex and cover glass and scanned with the light microscope (Q550IW; Leica, Germany) at 100x magnification using Leica QWin3 Standard and Leica QGo Routine Runner software yielding 50-100 images for each lobe (up to 300 per animal). Each of images was reviewed and degree of fibrosis was assigned according to Ashcroft's fibrosis score system [145] with slight modifications: normal lung was referred to as score 0 while score 6 represented maximal degree of pathological changes.

3.2.13. Collagen assay

Levels of acid-soluble collagens in lung tissues were determined by SIRCOL collagen assay (Biocolor Ltd., UK) according to manufacturer's instructions. Briefly, left lung lobes were homogenized and collagens were solubilized overnight in 0.5M acetic acid. Extracts were incubated with Sirius red dye for 30 min and centrifuged at

13000 rpm for 10 min to precipitate collgen-Sirus red complexes. Pellets were then dissolved in 0.5M sodium hydroxide and absorbance was determined at 540 nm with spectrophotometer Infinite M200 (Tecan, Austria). Soluble bovine skin type I collagen in amounts of 0 – 12.5 – 25 – 50 – 100 µg was used as a standard for calibration curve. Amount of collagen was calculated by accompanying Magellan software and expressed in µg/g of wet tissue.

3.2.14. Survival analysis

Survival of mice for each treatment group was expressed as percent of animals left of original number at the specific time points of the experiment. For creating staircase survival curve with GraphPad Prism® software “1” was referred to a death event while “0” was referred to a survival event (“censored”).

3.2.15. Data analysis

All data are expressed as means +/-SEM. One-way Analysis of Variance (ANOVA) test and Student-Newman-Keuls Post test were used for multiple comparisons and Mann-Whitney test was used for pairwise comparisons utilizing GraphPad Prism® software. A p-value less than 0.05 was considered statistically significant.

4. Results

4.1. Analysis of PDE4 expression in pulmonary fibrosis

To investigate the possible role of PDE4 in pulmonary fibrosis its expression was analyzed at mRNA and protein levels both in mice and humans.

Results of RT-qPCR performed on the lungs of mice with bleomycin-induced lung fibrosis showed time-dependent downregulation of all PDE4 genes (Fig. 9). Namely, at days 7 and 24 mRNA levels of PDE4A (ΔCt 10.31±0.13 and 10.38±0.16 at 7d and 24d), PDE4B (ΔCt 7.14±0.17 and 8.00±0.24 at 7d and 24d; $p<0.001$ for bleo 24d vs. saline), PDE4C (ΔCt 14.50±0.38 and 14.70±0.35 at 7d and 24d; $p<0.01$ for bleo 7d vs. saline and for bleo 24d vs. saline) and PDE4D (ΔCt 11.14±0.18 and 11.97±0.26 at 7d and 24d; $p<0.001$ for bleo 24d vs. saline) genes were decreased compared to mice received sterile saline only (ΔCt 9.58±0.18, 6.50±0.16, 13.53±0.30 and 10.23±0.28 for PDE4A, B, C and D respectively). Baseline expression was the highest for PDE4B gene and the lowest for PDE4C gene while equally moderate in case of PDE4A and PDE4D genes. PCR primers were designed to detect all isoforms within one PDE4 gene.

Expression of PDE4 analyzed with western blotting (Fig. 10) showed differential regulation at the protein level in the lungs with bleomycin-induced lung fibrosis. PDE4A isoforms 5, 8 and x were significantly downregulated (0.30±0.20 and 0.13±0.10 at 7d and 24d; $p<0.02$ for bleo 7d vs. saline and $p<0.02$ for bleo 24d vs. saline) compared to saline-treated mice (1.56±0.26) while expression of PDE4A1 isoform did not change. Expression of PDE4B isoform 1 was also decreased (0.79±0.12 and 0.52±0.05 at 7d and 24d) compared to controls (0.73±0.11). Interestingly, expression of PDE4B isoform 4 was significantly increased and peaked at day 7 after bleomycin administration (4.13±0.42 and 2.10±0.19 at 7d and 24d; $p<0.02$ for bleo 7d vs. saline) compared to controls (2.0±0.28).

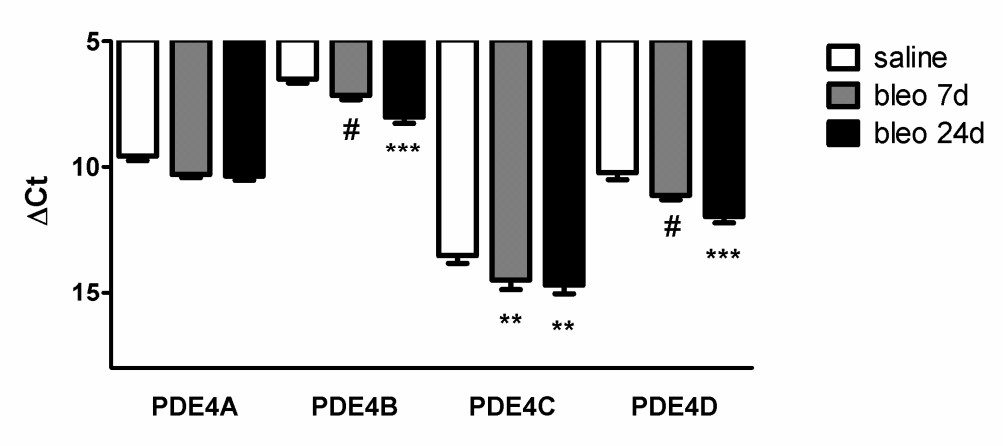

Fig. 9. Expression of PDE4 genes at mRNA level in mouse lungs: healthy mice ("saline") and mice suffering from fibrosis ("bleo") for 7 or 24 days after bleomycin administration. Real-Time RT-PCR data are normalized to β-actin expression and presented as ΔCt values ± SEM. * bleo vs. saline (** $p<0.01$, *** $p<0.001$), # bleo 7d vs. bleo 24d (# $p<0.05$). N=4 per group.

Expression of PDE4B isoforms 2 and 3 was at undetectable level. Expression of PDE4C isoform 2 was elevated (0.12±0.01 and 0.07±0.01 at bleo 7d and 24d; $p<0.05$ for bleo 7d vs. saline) compared to controls (0.06±0.01) while isoform 1 was undetectable. PDE4D isoforms 1/2 and 3 were downregulated both at 7 (0.18±0.03 and 0.20±0.02 respectively) and 24 days (0.12±0.02 and 0.16±0.02 respectively) after bleomycin administration while isoform 4 was slightly upregulated (0.13±0.03 and 0.16±0.01 at 7d and 24d) compared to healthy lungs (0.22±0.04, 0.21±0.11 and 0.10±0.03 for isoforms 1/2, 3 and 4 respectively). Baseline expression was the highest for PDE4A (isoforms 5, 8 and x) and PDE4B (isoforms 1 and 4) genes.

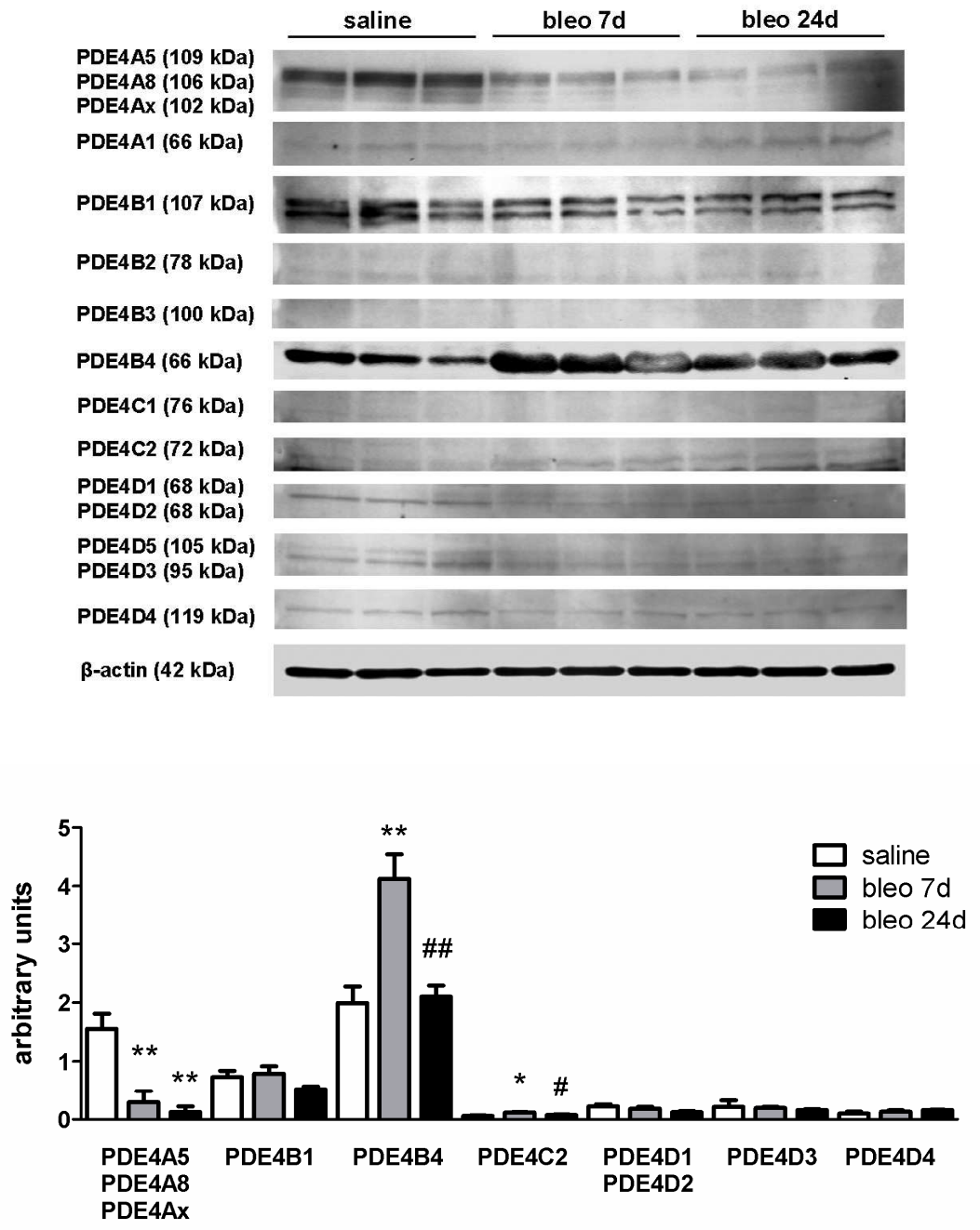

Fig. 10. Expression of PDE4 genes at protein level in mouse lungs: healthy mice ("saline") and mice suffering from fibrosis ("bleo") for 7 or 24 days after bleomycin administration. Upper part: western blotting autoradiographs, lower part: densitometry quantification. Densitometry data are normalized to β-actin expression and presented as arbitrary units ± SEM. * bleo vs. saline (*$p<0.05$, ** $p<0.01$), # bleo 7d vs. bleo 24d (# $p<0.05$, ## $p<0.01$). N=3 per group.

Analysis of PDE4 mRNA levels in the lungs of IPF patients (Fig. 11) showed downregulation of PDE4A (ΔCt 7.99±0.16) and PDE4D (ΔCt 8.75±0.19, $p<0.05$ vs. donor) in comparison to healthy donors (ΔCt 7.39±0.10 and 8.12±0.31 respectively). Expression of PDE4B and PDE4C genes did not differ between donors (ΔCt 9.30±0.10 and 9.16±0.26) and IPF patients (ΔCt 9.18±0.19 and 9.21±0.15 respectively). Baseline expression was higher for PDE4A and PDE4D genes than for PDE4B and PDE4C genes. PCR primers for human PDE4s were also designed to detect all isoforms within each PDE4 gene.

Fig. 11. Expression of PDE4 genes at mRNA level in human lungs: healthy donors or IPF patients. Real-Time RT-PCR data are normalized to β-actin expression and presented as ΔCt values ± SEM. * IPF vs. donor (* $p<0.05$). N=4 per group.

Western blotting results (Fig. 12) showed upregulation of PDE4A1 isoform in lungs of IPF patients (0.59±0.43 vs. 0.13±0.01 in donors) while isoforms 5, 8 and x were not detected. Among PDE4B genes only isoform 4 was detected and was upregulated in IPF lungs (0.28±0.08 vs. 0.23±0.07 in donors). Both PDE4C isoforms 1 and 3 were downregulated in case of IPF (0.09±0.03 and 0.09±0.02 respectively vs. 0.18±0.01 and 0.10±0.04 in donors). PDE4D isoform 4 was also downregulated in the lungs of IPF patients (0.87±0.06 vs. 0.98±0.13 in donors) while isoforms 1, 2 and 3 were not detected. Baseline expression was the highest in case of PDE4D4 isoform.

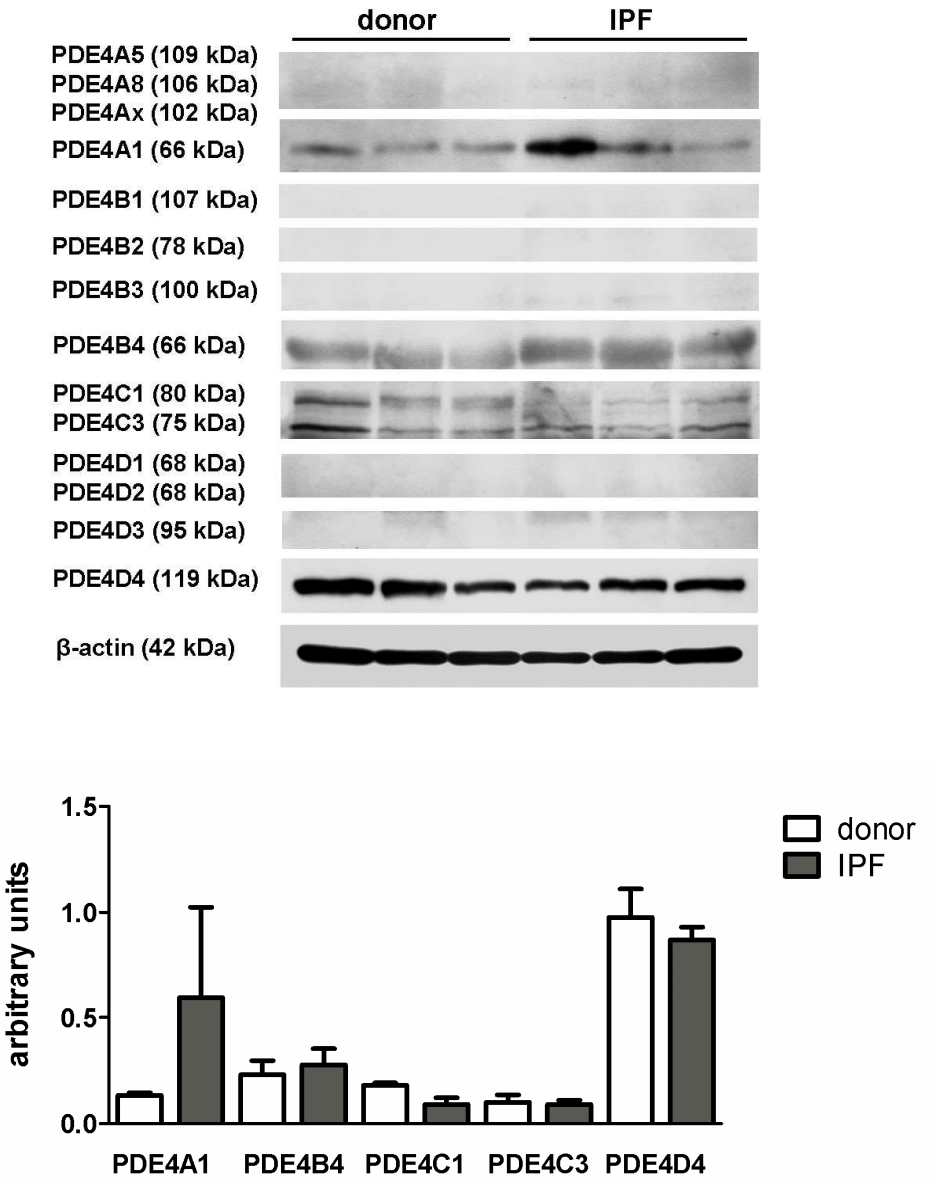

Fig. 12. Expression of PDE4 genes at protein level in human lungs: healthy donors or IPF patients. Upper part: western blotting autoradiographs, lower part: densitometry quantification. Densitometry data are normalized to β-actin expression and presented as arbitrary units ± SEM. N=3 per group.

4.2. Physiological effects of PDE4 inhibition

To evaluate possible side effects of cilomilast itself minimal pharmacological observations were carried out in healthy male C57BL/6N mice. Animals were treated *per os* once a day with vehicle (2% aqueous methylcellulose solution) or cilomilast suspended in vehicle at the doses of 10, 25, 50 and 100 mg/kg body weight. Body weight monitoring showed that doses higher than 50 mg/kg cause loss of body weight (Fig. 13). Moreover, such high doses caused increased motility manifesting itself as increased running speed, more frequent attempts to escape and resistance to necessary manipulations. No other side effects, such as vomiting or diarrhea, were observed. Similarly, no mortalities were observed in mice that were receiving any dose of cilomilast.

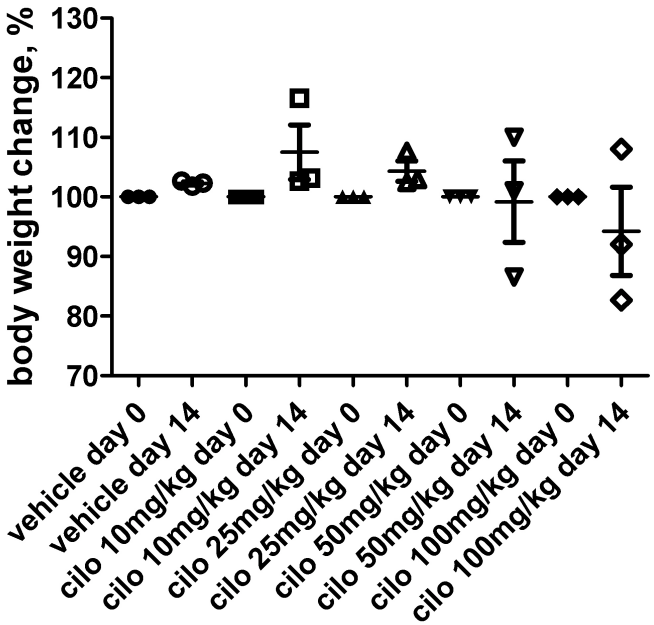

Fig. 13. Effect of PDE4 inhibition on body weight of healthy mice. Per cent of body weight change after 14 days of treatment with different doses of cilomilast. N=3 per group.

4.3. Effect of PDE4 inhibition on alveolar inflammatory cells content

To investigate the effect of cilomilast on early inflammatory stage of bleomycin-induced fibrosis, BALF was collected from healthy mice treated with vehicle and mice that received bleomycin and treated either with cilomilast or vehicle only. Total number of cells (3.1±0.4 x10^5 cells/ml in healthy controls) was highly increased by bleomycin instillation (11.9±1.8 x10^5 and 11.2±0.8 x10^5 cells/ml at 4d and 7d respectively) and was significantly ($p<0.001$ and $p<0.05$) lowered by cilomilast both at 4 and 7 days (5.5±0.5 x10^5 and 7.6±0.2 x10^5 cells/ml respectively) (Fig. 14).

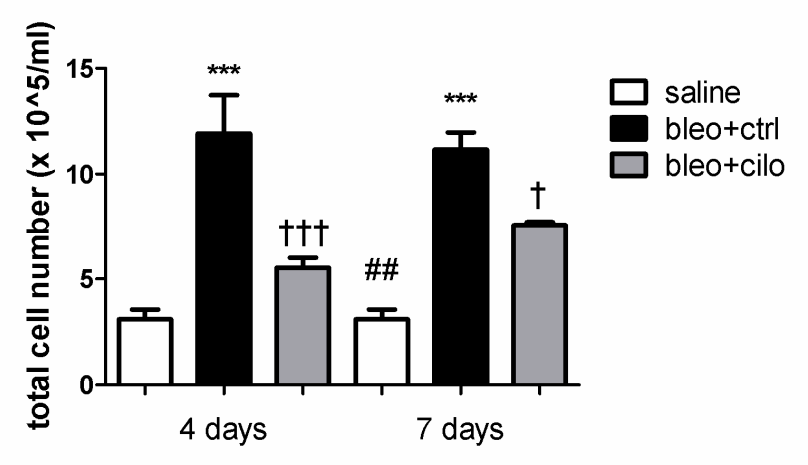

Fig. 14. Effect of PDE4 inhibition on BALF total cell number: healthy mice ("saline") and mice suffering from fibrosis and treated either with vehicle ("bleo+ctrl") or cilomilast ("bleo+cilo") at days 4 and 7 after bleomycin instillation. Values are presented as means ± SEM. * bleo+ctrl vs. saline (*** $p<0.001$), † bleo+cilo vs. bleo+ctrl († $p<0.05$, ††† $p<0.001$), # bleo+cilo vs. saline (## $p<0.01$). N=6 per group.

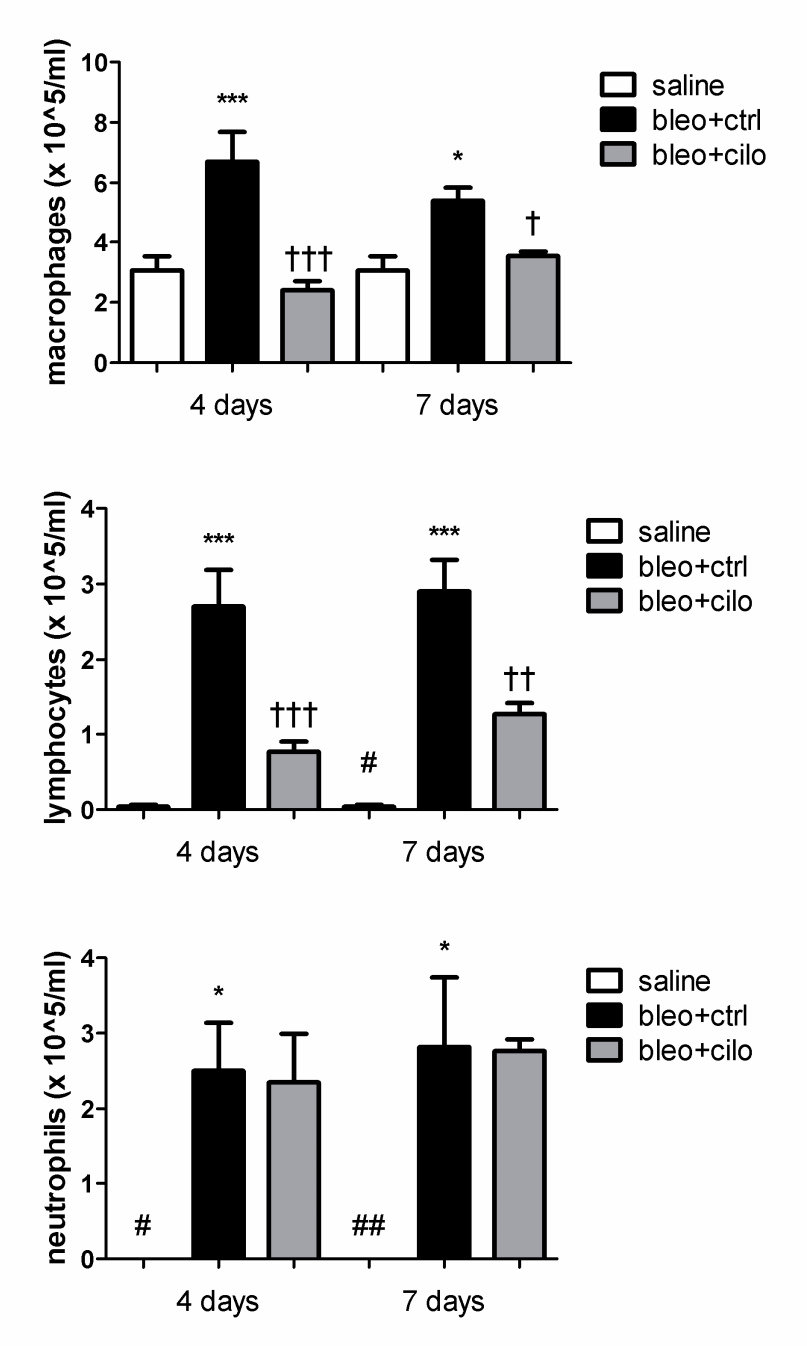

Fig. 15. Effect of PDE4 inhibition on number of macrophages, lymphocytes and neutrophils in BALF: healthy mice ("saline") and mice suffering from fibrosis and treated either with vehicle ("bleo+ctrl") or cilomilast ("bleo+cilo") at days 4 and 7 after bleomycin instillation. Values are presented as means ±SEM. * bleo+ctrl vs. saline (*p<0.05, ***p<0.001), † bleo+cilo vs. bleo+ctrl († p<0.05, †† p<0.01, ††† p<0.001), # bleo+cilo vs. saline (# p<0.05, ## p<0.01). N=6 per group.

To further evaluate the action of cilomilast on different inflammatory cell types differential cell count was performed (Fig. 15). As expected, influx of all cell types in alveolar space was prominent (macrophages: 6.7±1.0 x10^5 and 5.4±0.4 x10^5 cells/ml at 4d and 7d vs. 3.0±0.5 x10^5 cells/ml), with the highest increase in number of lymphocytes (2.7±0.5 x10^5 and 2.9±0.4 x10^5 cells/ml at 4d and 7d vs. 0.04±0.02 x10^5 cells/ml) and neutrophils (2.5±0.6 x10^5 and 2.8±0.9 x10^5 cells/ml at 4d and 7d vs. 0.0068±0.0062 x10^5 cells/ml). Number of macrophages (2.4±0.3 x10^5 and 3.6±0.1 x10^5 cells/ml at 4d and 7d) and lymphocytes (0.8±0.1 x10^5 and 1.3±0.1 x10^5 at 4d and 7d) was significantly decreased by cilomilast ($p<0.001$ and $p<0.05$ respectively). Number of neutrophils, however, remained unchanged (2.4±0.6 x10^5 and 2.8±0.2 x10^5 cells/ml at 4d and 7d).

4.4. Effect of PDE4 inhibition on lung inflammatory markers

To evaluate expression of inflammatory markers after cilomilast treatment, lung homogenate RT-qPCR was carried out at the same time points as for BALF cell count. TNFα and IL1β expression was significantly elevated at 4 and 7 days after bleomycin instillation (ΔCt 11.18±0.15 and 11.05±0.14 at 4d and 7d for TNFα; ΔCt 9.24±0.41 and 9.44±0.24 at 4d and 7d for IL1β) compared to those in animals that received saline (ΔCt 13.74±0.12 and 10.46±0.09 respectively) (Fig. 16, 17). Treatment with cilomilast resulted in significantly ($p<0.01$ at 4d and $p<0.001$ at 7d) lower TNFα level (ΔCt 12.03±0.18 and 12.37±0.10 at 4d and 7d), but not in IL1β (ΔCt 8.22±0.79 and 9.07±0.19 at 4d and 7d) mRNA levels compared to mice treated with vehicle only.

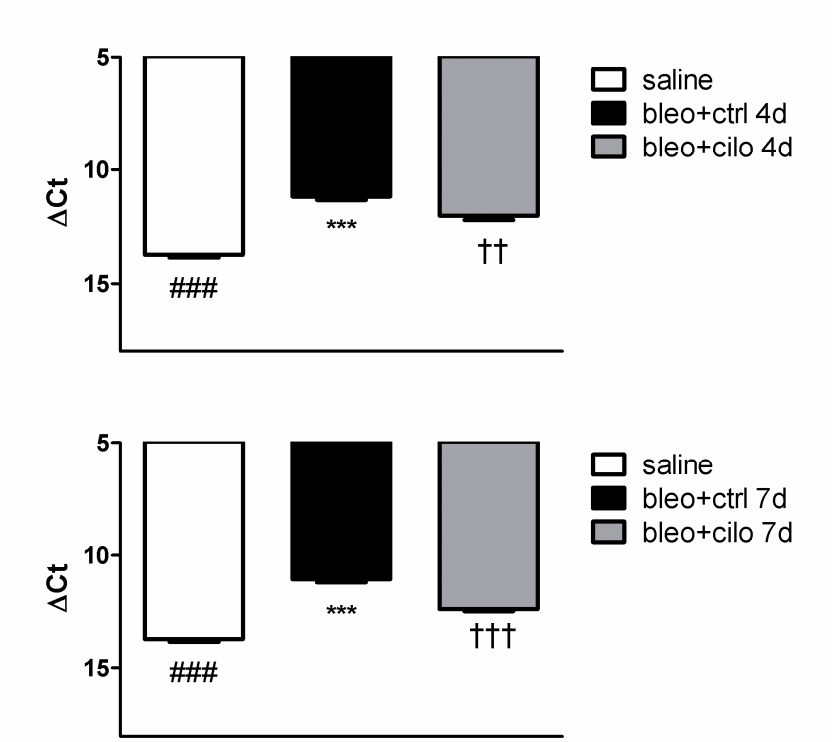

Fig. 16. Effect of PDE4 inhibition on lung TNFα levels: healthy mice ("saline") and mice suffering from fibrosis and treated either with vehicle ("bleo+ctrl") or cilomilast ("bleo+cilo") at days 4 and 7 after bleomycin administration. Real-Time RT-PCR data are normalized to β-actin expression and presented as ΔCt values ±SEM. * bleo+ctrl vs. saline (***$p<0.001$), † bleo+cilo vs. bleo+ctrl (†† $p<0.01$, ††† $p<0.001$), # bleo+cilo vs. saline (### $p<0.001$). N=6 per group.

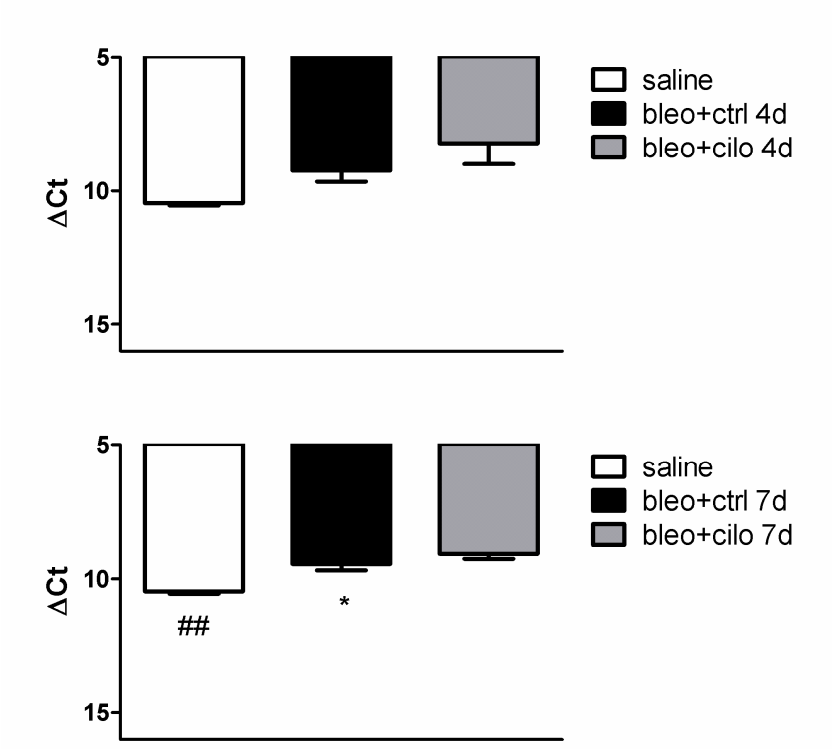

Fig. 17. Effect of PDE4 inhibition on lung IL1β levels: healthy mice ("saline") and mice suffering from fibrosis and treated either with vehicle ("bleo+ctrl") or cilomilast ("bleo+cilo") at days 4 and 7 after bleomycin administration. Real-Time RT-PCR data are normalized to β-actin expression and presented as ΔCt values ±SEM. * bleo+ctrl vs. saline (* $p<0.05$), # bleo+cilo vs. saline (## $p<0.01$). N=6 per group.

Level of IL6 mRNA (Fig. 18) was also significantly elevated by bleomycin both at 4 (ΔCt 15.51±0.30) and 7 days (ΔCt 15.38±0.30) compared to one in mice received saline (ΔCt 19.17±0.49). Interestingly, in cilomilast-treated animals IL6 expression was significantly increased (ΔCt 12.98±1.10 and ΔCt 13.67±0.42 at 4d and 7d; $p<0.05$ and $p<0.01$ respectively).

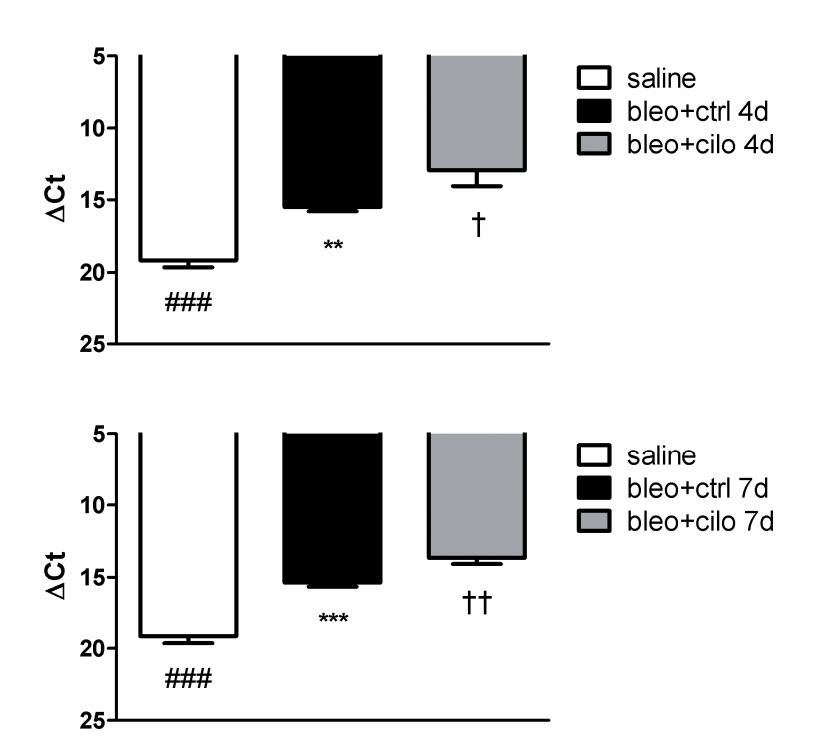

Fig. 18. Effect of PDE4 inhibition on lung IL6 levels: healthy mice ("saline") and mice suffering from fibrosis and treated either with vehicle ("bleo+ctrl") or cilomilast ("bleo+cilo") at days 4 and 7 after bleomycin administration. Real-Time RT-PCR data are normalized to β-actin expression and presented as ΔCt values ±SEM. * bleo+ctrl vs. saline (** $p<0.01$, *** $p<0.001$), † bleo+cilo vs. bleo+ctrl († $p<0.05$, †† $p<0.01$), # bleo+cilo vs. saline (### $p<0.001$). N=6 per group.

4.5. Effect of PDE4 inhibition on lung function

To examine the effect of cilomilast on late stage fibrosis, lung compliance (Fig. 19) was evaluated in animals treated either with cilomilast or vehicle alone, as well as in mice received instillation of sterile saline and treated with vehicle. Pulmonary compliance was significantly decreased in animals with bleomycin-induced fibrosis, both at 14 and 24 days (0.09±0.006 and 0.06±0.007 ml/kPa vs. 0.17±0.01 and 0.17±0.003 ml/kPa) suggesting lower elasticity of the lung. Treatment

with cilomilast partially restored impaired lung function (0.11±0.003 and 0.08±0.006 ml/kPa at 14d and 24d) compared to mice treated with vehicle alone, with improvement being significant at 14 days ($p<0.05$).

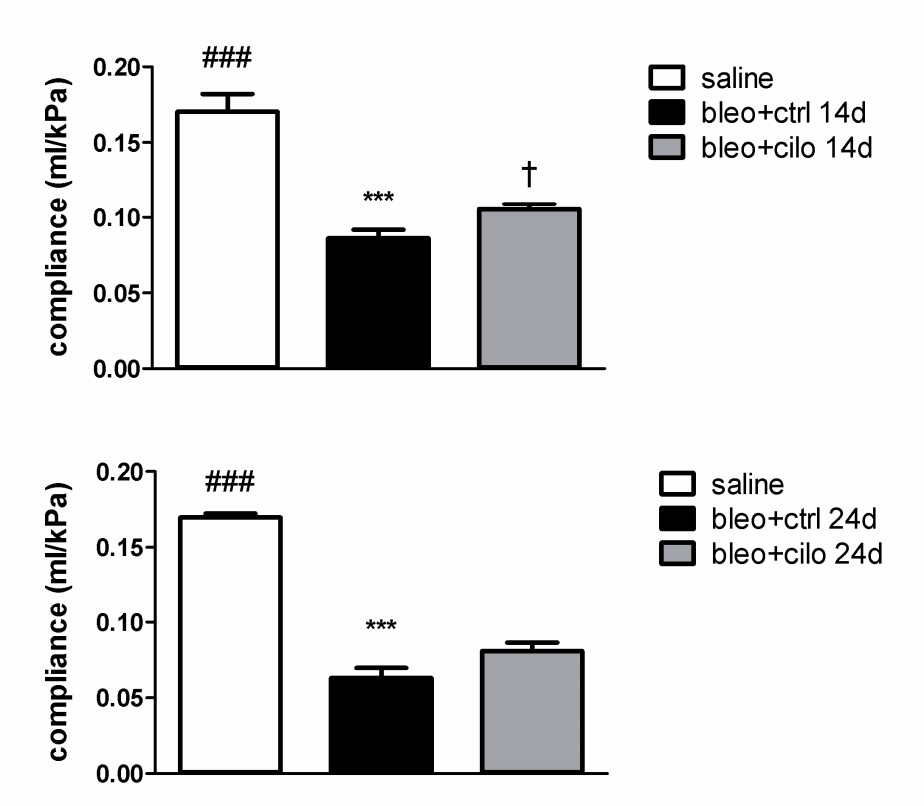

Fig. 19. Effect of PDE4 inhibition on lung compliance: healthy mice ("saline") and mice suffering from fibrosis and treated either with vehicle ("bleo+ctrl") or cilomilast ("bleo+cilo") at days 14 and 24 after bleomycin administration. Values are presented as means ± SEM. * bleo+ctrl vs. saline (*** $p<0.001$), † bleo+cilo vs. bleo+ctrl († $p<0.05$), # bleo+cilo vs. saline (### $p<0.001$). N=9 per group.

When normalized to body weight (Fig. 20) similar results were obtained: lung compliance was significantly decreased by bleomycin (0.0050±0.0003 and 0.0031±0.0003 (ml/kPa)/g at 14d and 24d) compared to one of healthy mice (0.0069±0.0007 and 0.0089±0.0003 (ml/kPa)/g respectively). Treatment with

cilomilast resulted in significant increase in lung compliance both at 14d and 24d (0.0069±0.0004 and 0.0041±0.0003 (ml/kPa)/g; $p<0.01$ and $p<0.05$ respectively).

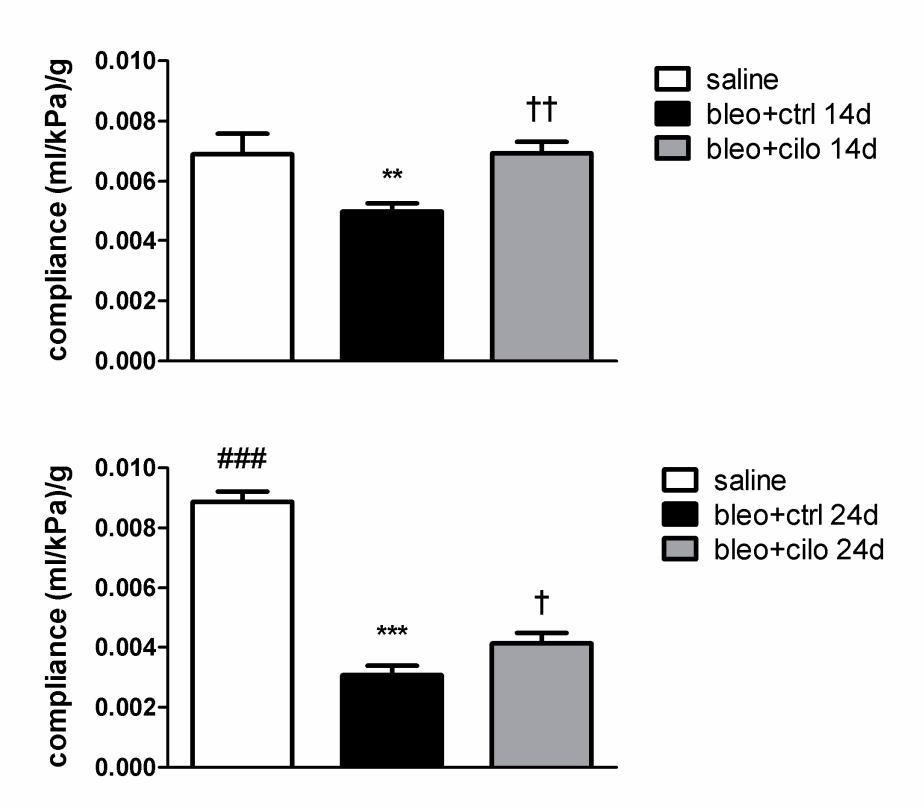

Fig. 20. Effect of PDE4 inhibition on lung compliance (normalized): healthy mice ("saline") and mice suffering from fibrosis and treated either with vehicle ("bleo+ctrl") or cilomilast ("bleo+cilo") at days 14 and 24 after bleomycin administration. Values are presented as means ± SEM. * bleo+ctrl vs. saline (** $p<0.01$, *** $p<0.001$), † bleo+cilo vs. bleo+ctrl († $p<0.05$, †† $p<0.01$), # bleo+cilo vs. saline (### $p<0.001$). N=9 per group.

4.6. Effect of PDE4 inhibition on lung pathology

To confirm the mentioned findings and directly investigate pathological changes in the lungs quantified fibrosis degree estimation was performed by means of microscopy followed by scoring (Fig. 21). High scores obtained from the lungs with

bleomycin-induced fibrosis (3.50±0.15 and 3.69±0.15 at 14d and 24d vs. 0.34±0.05) evidenced significant distortion of lung architecture. However, generally lower fibrosis degree was observed in animals treated with PDE4 inhibitor (3.18±0.14 and 3.03±0.19 at 14d and 24d) compared to ones treated with vehicle only, reaching significance at day 24 ($p<0.05$).

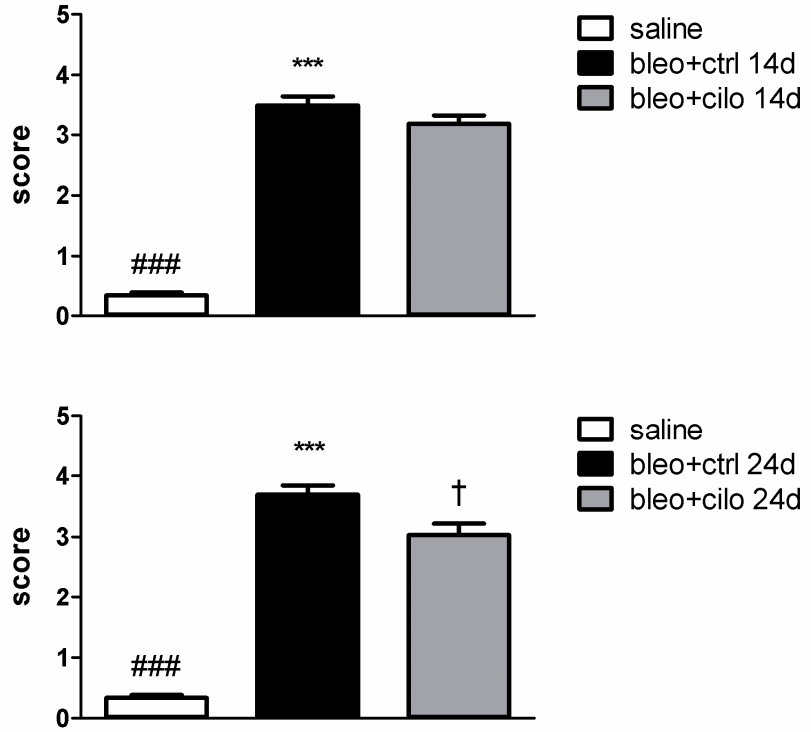

Fig. 21. Effect of PDE4 inhibition on lung pathology scoring: healthy mice ("saline") and mice suffering from fibrosis and treated either with vehicle ("bleo+ctrl") or cilomilast ("bleo+cilo") at days 14 and 24 after bleomycin administration. Values are presented as means ± SEM. * bleo+ctrl vs. saline (*** $p<0.001$), † bleo+cilo vs. bleo+ctrl († $p<0.05$), # bleo+cilo vs. saline (### $p<0.001$). N=9 per group.

Representative images of lung sections (Fig. 22) stained with Hematoxilin-Eosin illustrate the mentioned pathological changes quantified by fibrosis scoring.

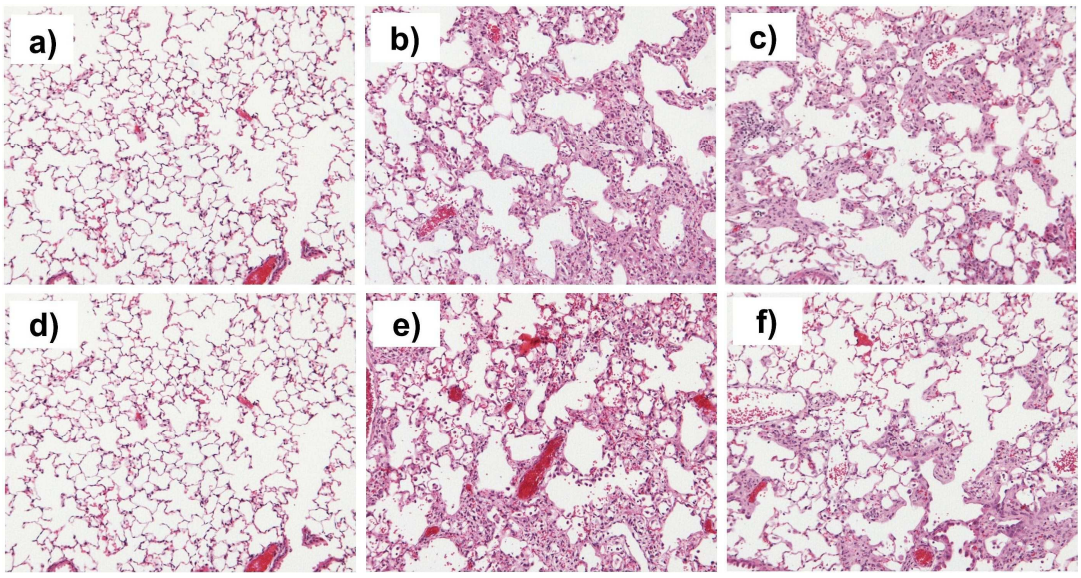

Fig. 22. Representative images of PDE4 inhibition effect on lung pathology: histological pictures of lungs of healthy mice (a, d) and of mice suffering from fibrosis and treated either with vehicle (b, e) or cilomilast (c, f) at days 14 (a, b, c) and 24 (d, e, f) after bleomycin administration. Hematoxilin-Eosin staining, magnification x100. N=9 per group.

4.7. Effect of PDE4 inhibition on lung collagen content

Total soluble collagen content in the lungs was estimated by SIRCOL assay 24 days after bleomycin instillation (Fig. 23), when changes in collagen content are the most distinctive. Indeed, the 2-fold increase (1639±98 vs. 740±42 μg/g) was observed among the mice received bleomycin. In contrast, animals treated with cilomilast tended to demonstrate lower collagen content in the lungs (1490±30 μg/g).

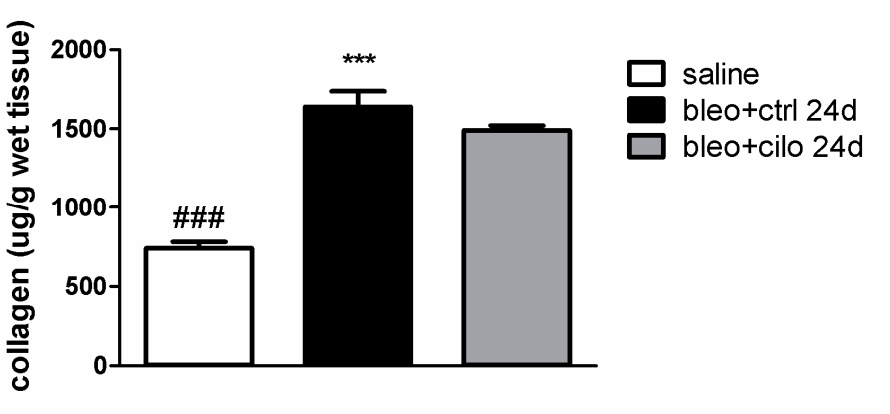

Fig. 23. Effect of PDE4 inhibition on lung collagen content: healthy mice ("saline") and mice suffering from fibrosis and treated either with vehicle ("bleo+ctrl") or cilomilast ("bleo+cilo") at day 24 after bleomycin administration. Values are presented as means ± SEM. * bleo+ctrl vs. saline (*** $p<0.001$), # bleo+cilo vs. saline (### $p<0.001$). N=4 per group.

4.8. Effect of PDE4 inhibition on survival

General effect of cilomilast on the course of experimental PF was evaluated with the survival curves (Fig. 24). As expected, shorter experiment (14 days) resulted in less mortality compared to longer (24 days) one (88.9% and 43.8% survival at 14d and 24d vs. 100%). In both cases slightly higher survival rate (100% and 66.7% at 14d and 24d) was observed in the groups received PDE4 inhibitor.

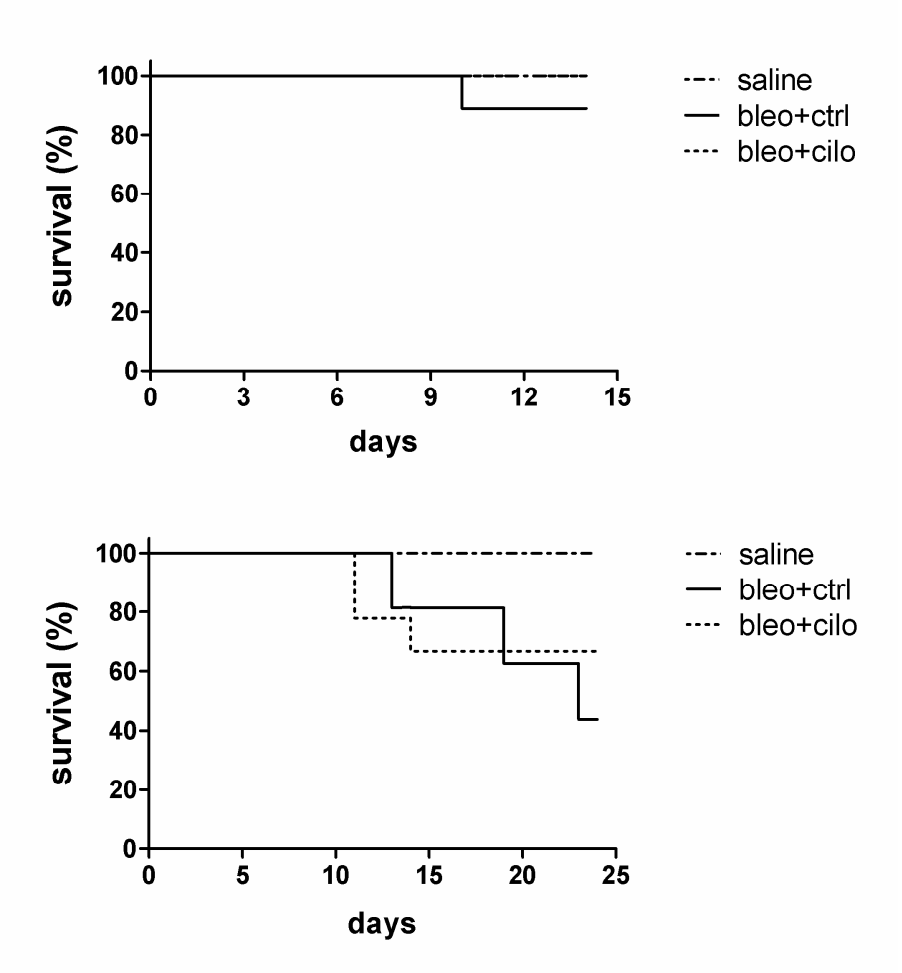

Fig. 24. Effect of PDE4 inhibition on survival: healthy mice ("saline") and mice suffering from fibrosis and treated either with vehicle ("bleo+ctrl") or cilomilast ("bleo+cilo") followed up for 14 and 24 days after bleomycin instillation. Kaplan-Meier curves. N=9 per group.

5. Discussion

5.1. Bleomycin-induced pulmonary fibrosis

Pulmonary fibrosis represents a number of interstitial lung diseases (ILD) and usual interstitial pneumonia (UIP), indicating chronic interstitial inflammation, is the most common histopathological characteristic [4,22]. Similarly, bleomycin-induced lung fibrosis possesses classical inflammatory pattern and is the most common model for PF [54,62].

However, some limitations of the animal model described in the literature were observed in the present work as well. For instance, classical fibroblast foci were hardly present in remodeled tissues. On the other hand, remodeling during experimental PF involved inflammatory cell infiltration to a greater degree than in case of human IPF. Susceptibility of mice to bleomycin varied within the groups what could be accounted to individual biochemical profiles. Similarly, often described self-resolution of bleomycin-induced PF was not observed in most of experiments. Survival of an animal at 3, 4 or 5 weeks after PF induction was mediated more by lesser degree of fibrosis developed in the particular animal rather than by self-resolution of PF.

5.2. Expression of PDE4 in pulmonary fibrosis

PDE4 plays important role in cellular homeostasis and, in particular, in such processes as proliferation and differentiation. Therefore, it was of interest to uncover the expression of PDE4 genes and their isoforms in the lungs with both experimental and human PF.

In the lungs of mice all four PDE4 genes A, B, C and D were time-dependently downregulated at mRNA level during the course of experimental PF.

Interestingly, PDE4B was the most abundant in healthy mouse lungs, while PDE4C was the least abundant one. PDE4A and PDE4D were expressed at relative moderate level. PDE4 genes were differently regulated at the protein level. In this case, baseline expression was the highest for PDE4A (isoforms 5, 8 and x) and PDE4B (isoforms 1 and 4) genes. The latter, therefore, matches the result of RT-qPCR indicating high basal PDE4B expression in mouse lungs. During bleomycin-induced PF PDE4A (isoforms 5, 8 and x) and PDE4B (isoform 1) were downregulated, while PDE4B isoform 4 was heavily upregulated, with the peak at 7d after PF induction. PDE4C2 was upregulated and PDE4D isoform 4 were slightly upregulated while PDE4D isoforms 1/2 and 3 were downregulated at the protein level.

When human donor lungs were analyzed baseline expression was higher for PDE4A and PDE4D genes than for PDE4B and PDE4C at mRNA level. In IPF lungs PDE4A and PDE4D were downreglated while expression of PDE4B and PDE4C was not any different compared to healthy donors. At the protein level baseline expression was the highest in case of PDE4D4, therefore matching the results of RT-qPCR. Under IPF conditions, PDE4A isoform 1 was slightly upregulated. As in case of experimental PF, isoform 4 of PDE4B was upregulated in IPF lungs. Both isoforms of PDE4C were downregulated, as well as isoform 4 of PDE4D gene.

It was surprising to see differential, if not opposite, regulation of PDE4 genes in mice and humans under pathological conditions at the protein level. As such, PDE4A was downregulated in mouse PF but upregulated in IPF. Limited number of reports shows that PDE4A is present in the lung and T-cells but lacks in neutrophils [95,102] therefore the mentioned changes could not be mediated by differences in neutrophil infiltration status.

PDE4C gene was upregulated at protein level during experimental fibrosis but downregulated in IPF lungs. Although expression of PDE4C variants is not fully understood, it is known that PDE4C is present in the lung but absent from circulating inflammatory cells [97-98,119]. Therefore, its upregulation in bleomycin-induced PF is not associated with ongoing inflammation as one could expect.

PDE4D was in general downregulated both at mRNA and protein level in both mice and humans. Besides lung tissue and T-cells [93,102,114] PDE4D is

present in well-differentiated human bronchial epithelium (WD-HBE) cells [99]. Extensive remodeling occurring during fibrosis ultimately leads to substitution of original tissue by masses of connective tissue. In this view, decreased levels of PDE4D mRNA and protein may be accounted for epithelium loss during PF development.

Most notably, PDE4B was upregulated at protein level in lungs of both in mice and humans suffering from PF. In particular, protein level was heavily increased at day 7 of experimental fibrosis, when inflammatory response to bleomycin is the main characteristic. Besides the lung, PDE4B is highly expressed in inflammatory cells, including monocytes, lymphocytes and neutrophils, where it is the major cAMP-hydrolyzing enzyme [95,100-102]. Finally, it was showed that PDE4B is required for recruitment, activation and proliferation of T-cells [119-120] as well as for TNFα production and development of inflammatory response by leukocytes and macrophages [104-105,118]. Thus, the data shown confirm the observations made by other authors.

5.3. Inhibition of PDE4 *in vivo*

PDE4 is the major class of PDEs expressed in inflammatory cells [95]. Chronic interstitial inflammation is the most common pathological characteristic both in human and experimental PF. Therefore we suggested application of a selective PDE4 inhibitor to mainly affect interstitial inflammation and investigate its other possible effects.

The dose of cilomilast was based on reports with 30 mg/kg successfully used in mice. However the dose range was as broad as 1-100 mg/kg for mice [134] and 0.1-100 mg/kg for rats [136]. Our own minimal pharmacological observations showed that the dose of 50 mg/kg was a compromise between therapeutic efficiency and drug toxicity. Higher PDE4 inhibitor doses caused loss of body weight and increased physical activity in healthy animals. In the latter case, direct CNS effects of

cilomilast cannot be excluded as PDE4D gene is expressed in cortex and cerebellum where it is involved in α2A-adrenoceptor signaling in neurons [126]. Thus, dose of 50 mg/kg was primarily used in the present work. Higher dose (100 mg/kg) was also used for treatment of experimental PF. However, treatment effects were similar to those of 50 mg/kg dose suggesting that further dose increase does not lead to increased therapeutic effect.

5.4. Effects of PDE4 inhibition on inflammatory cell influx

Given that PDE4 is the major cAMP hydrolyzing enzyme in inflammatory cells, including monocytes, lymphocytes and neutrophils, strong effects of PDE4 inhibitor on these cells could be expected. Indeed, the total cell number in BALF of mice treated with cilomilast was significantly reduced at the early stage of bleomycin-induced pulmonary fibrosis. Numbers of macrophages and lymphocytes were significantly decreased as well. Interestingly, we could observe that increase in total cell number (3.5-4-fold) by bleomycin was accounted mostly for macrophages, as they represent the largest defense cell population in alveolus. On the other hand, although absolute number of lymphocytes and neutrophils was relatively low, increase in number of these cell types was about 30-fold for lymphocytes and about 400-fold for neutrophils. Similar results are observed both in humans and mice with pulmonary fibrosis [13,59]. However it was unexpected to see no significant effect of cilomilast on number of neutrophils, which conflicts with other similar studies. For instance, Corbel et al. [135] could demonstrate the decrease in neutrophils release by selective PDE4 inhibitor PR 73-401 (piclalmilast) in a murine model of LPS-induced acute inflammation. Similar effects have been observed by other authors [136].

Neutrophils play important role in inflammatory processes and pathological tissue remodeling releasing primary (eg. elastase and myeloperoxydase, MPO) and secondary (eg. collagenase and lactoferrin) granule enzymes, as well as high concentrations of oxidants. Neutrophil elastase (NE), in turn, can induce MMPs

activation and, as a result, damage of lung parenchyma. Indeed, it was shown that IPF (also known as cryptogenic fibrosing alveolitis, CFA) patients have higher numbers of neutrophils and higher concentrations of proteolytic granule enzymes, such as MPO, collagenase, NE, lactoferrin in BALF [12], as well as increased NE levels in plasma and lung tissue [14]. Inability to influence neutrophils release therefore reveals potential limitations of the inhibitor used. It is worth noting, however, that different inhibitors were used in different studies. It is well documented that different substances possess different effects on cell types and mediators released. In example with PDE4 inhibitors, a study [136] shows differential potential of number of PDE4 inhibitors on neutrophils and TNFα release, indeed showing some limitations of cilomilast in particular.

5.5. Effects of PDE4 inhibition on the expression of inflammatory markers

It was interesting to see whether general suppression of inflammatory cells influx was also reflected in inflammatory cytokines expression throughout the lung at the same time points. Such genes as TNFα, IL1β and IL6 are known to be upregulated in the lugs of patients with PF [15-21]. TNFα and IL1β are also the canonical early inflammatory markers of experimental PF becoming upregulated in the first 4-7 days after bleomycin administration [39,59-60,64].

Indeed, expression of TNFα was significantly elevated upon bleomycin lung injury. It was significantly decreased in mice treated with cilomilast compared to non-treated ones both at 4 and 7 days after bleomycin administration. It is well known that macrophages, along with type II alveolar epithelial cells, represent the major source of TNFα [16]. Therefore, it was expected to see the downregulation of this cytokine after significant attenuation of macrophages influx by cilomilast that was demonstrated in BALF cell count experiments. Similar results were also showed by other authors [134].

Expression of IL1β was also significantly elevated at the early stage of experimental PF. However, cilomilast had no significant effect the level of this cytokine. Althouth other authors also observed the same result [146], it was a surprising finding as to a large extent IL1β is also produced by macrophages which numbers were decreased by cilomilast [16]. It is interesting to note that although expression of IL1β is well known to be elevated both in human and experimental PF its role in the remodeling process is controversial. As such, IL1β was shown to stimulate proliferation of fibroblasts and their production of collagen types 1 and 3 [28]. However, other reports show the opposite regulation of fibroblasts by this cytokine. For instance, IL1β could also decrease expression of α-smooth muscle actin in fibroblasts and induce their apoptosis through nitric oxide (NO) [147].

Similarly to TNFα and IL1β expression of IL6 was also significantly elevated at 4 and 7 days after bleomycin administration, which is also observed in the lungs of IPF patients [15,17,19-20]. Treatment with cilomilast caused further significant increase in IL6 expression. We suggest that increased expression of IL6 in experimental and human PF might be accounted to anti-fibrotic action of this factor. Indeed, it was shown that exogenous administration of IL6 decreased BALF cell recruitment, macrophage-mediated TNFα production and hydroxyproline content in experimental pneumonitis in mice [31]. Besides, IL6 can also be induced in fibroblasts by co-stimulation with pro-inflammatory cytokines TNFα and IL1β [28]. Although other authors showed pro-inflammatory action of IL6 [32], we believe that increase in IL6 expression observed after treatment with the PDE4 inhibitor accompanies the general suppression of inflammatory cell influx and TNFα content in the lung.

5.6. Effects of PDE4 inhibition on late stage fibrosis

With the progression of fibrosis, pathological changes become more obvious leading to further inflammatory cells infiltration and accumulation of connective

tissue leading to impairment of lung function. At first, this includes inability to maintain normal gas exchange as a conclusion of thickened interstitium. At second, as fibrosis goes on, worsening of lung mechanical properties occurs due to increasing stiffness of the tissue. The latter could be examined by means of pulmonary compliance measurement.

As expected, decreased compliance was observed in bleomycin-challenged mice. Similarly a higher degree of fibrosis was documented after histological examination of lungs of these animals, confirming compliance measurement results. Compliance was lower and score was higher at day 24 compared to day 14, illustrating progression of the disease. In addition, typical manifestation of bleomycin-induced lung fibrosis, such as its patchy pattern and substantial degree of inflammation were documented.

Animals treated with cilomilast demonstrated significantly higher lung compliance at 14 days after bleomycin instillation compared to non-treated ones whereas pathological changes occurring by day 24 were possibly more difficult to affect. It is important to note that the lung compliance values are not only influenced by the lung elasticity but also by the chest resistance. The latter, depends on the size of an animal that, in turn, is a function of body weight. Therefore, to minimize the possible artifacts compliance values were also normalized to body weight. The results not only remained similar but the level of the statistical significance rose as well.

Degree of pathological changes reflected in fibrosis scores was also less in the cilomilast-treated animals in a number of repetitive experiments. However, the improvements were not as prominent and did not always reach the level of statistical difference suggesting consistent but mild effect of PDE4 inhibition on late stage fibrosis.

5.7. Possible mechanisms of anti-fibrotic action of PDE4 inhibitors

Action of PDE4 inhibitor on tissue remodeling might have several aspects. First, selective inhibition of PDE4 is able to suppress inflammation effectively raising cAMP level and thereby eliminating pro-fibrotic environment in the tissue (Fig. 25, left). Indeed, cAMP suppresses TLR signaling pathway and LPS- and TNFα-induced inflammatory response [104-105]. Inflammatory cells also express markers, such as TNFα, IL1β, TGFβ and PDGF that are known to promote tissue remodeling. As such, TNFα levels are elevated in IPF lungs and it is able to directly stimulate the proliferation of lung fibroblasts [15,29]. In the present work we could demonstrate that PDE4 inhibitor decreased numbers of macrophages and lymphocytes and lowered TNFα expression in the lung. Interestingly, inhibition of TNFα by its soluble receptor alone can be sufficient to attenuate pulmonary fibrosis in mice [30].

On the other hand, there are some evidences that PDE4 inhibitors are able to act through inflammation-independent ways (Fig. 25, right). cAMP elevated by PDE4 inhibitors, PGE2 or AC stimulation inhibits lung fibroblast migration, proliferation, and collagen synthesis [106-108,139], as well as differentiation into myofibroblasts [109-110]. Similarly, cAMP inhibits proliferation of heart fibroblasts [141] and PASMCs [142]. Finally, PDE4 inhibitor directly attenuated fibroblast to miofibroblast transition, stimulated by TGFβ in inflammation-free environment [110]. Our group has also previously demonstrated that cAMP raised by PDE3/4 inhibitor tolafentrine inhibited enhanced migration of PASMCs that were derived from vessels of rats suffering from pulmonary hypertension [144]. Inhibition of PDE4 by cilomilast also suppresses release and activation of MMP1, MMP2 and MMP9 from human lung fibroblasts [98,143].

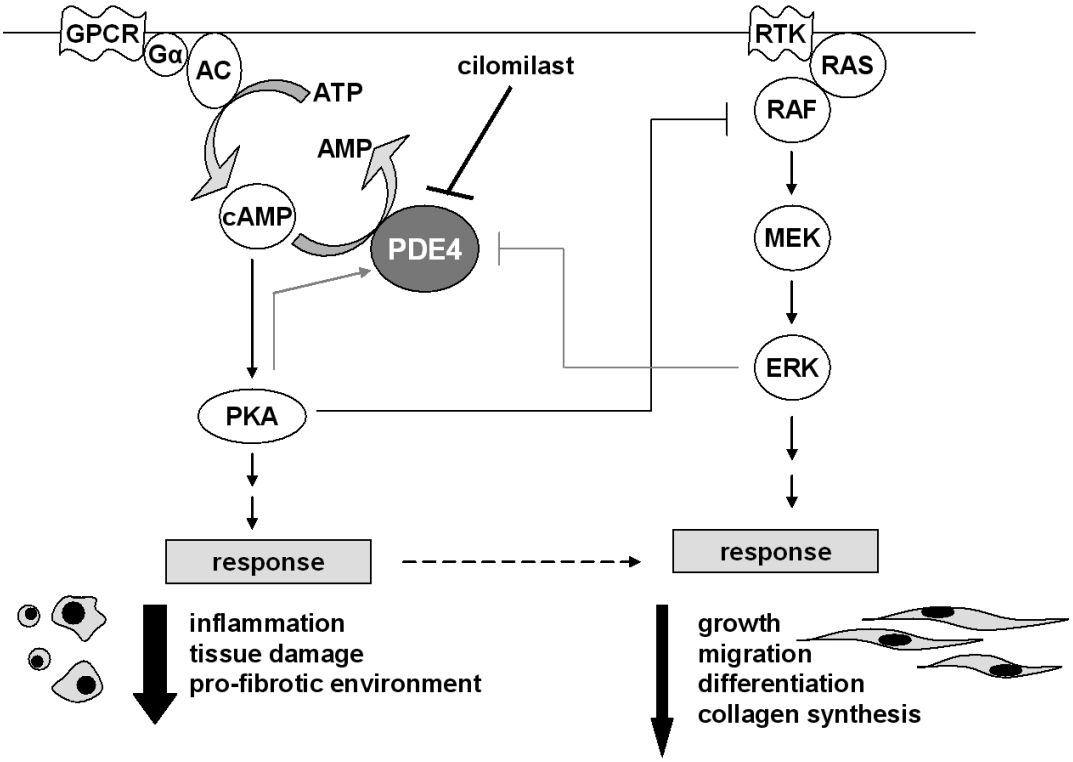

Fig. 25. Possible mechanism of anti-fibrotic action of PDE4 inhibitor: inflammation and remodeling branches, cross-talk between cAMP/PKA and MEK/ERK pathways and the molecules known to be involved.

Moreover, it was discovered, that PDE4B, 4C and 4D proteins contain conserved motifs for phosphorylation by extracellular signal-regulated kinase (ERK), thereby integrating AC/cAMP/PDE4/PKA and RAS/RAF/MEK/ERK pathways [85]. Although it was proved that ERK-mediated phosphorylation inhibits PDE4 recent data suggest that PKA can directly inhibit c-Raf and, therefore, the whole ERK pathway. The details of this interaction are not fully understood, however at least three possible mechanisms are suggested [111]. Thus, PDE4 inhibition, leading to cAMP elevation, might directly inhibit proliferation and cell growth resulting in attenuation of fibrosis and tissue remodeling in general. Hypothetical mechanism of anti-remodeling action of a PDE4 inhibitor is represented in the figure (Fig. 25).

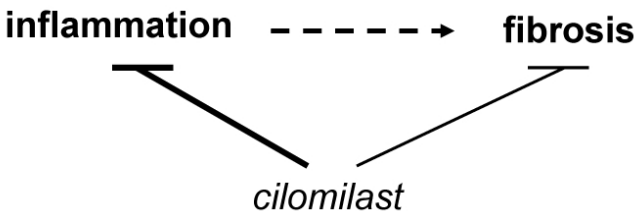

Fig. 25. Possible mechanism of anti-fibrotic action of PDE4 inhibitor (simplified): cilomilast affects fibrosis largely by suppressing inflammation and to some extent the remodeling itself.

All together these data suggest that the effects observed in present study might be accounted to several independent actions of the PDE4 inhibitor, affecting both inflammation process and the effector cells in the sites of fibrosis (Fig. 26). This, therefore, may open another possible therapeutic option for patients with pulmonary fibrosis.

6. References

1. Pulmonary Fibrosis Foundation. Patient Information Handbook. www.pulmonaryfibrosis.org. Last time updated: June 27, 2008. Last time accessed: December 18, 2008

2. American Thoracic Society. Idiopathic pulmonary fibrosis: diagnosis and treatment. International consensus statement. Am J Respir Crit Care Med 2000; 161: 646-64

3. Dempsey OJ, Kerr KM, Gomersall L, Remmen H, Currie GP. Idiopathic pulmonary fibrosis: an update. Q J Med 2006; 99: 643–654

4. American Thoracic Society/European Respiratory Society international multidisciplinary consensus classification of the idiopathic interstitial pneumonias. Am J Respir Crit Care Med 2002; 165: 277-304

5. Coultas DB, Zumwalt RE, Black WC, Sobonya RE. The epidemiology of interstitial lung diseases. Am J Respir Crit Care Med 1994; 150: 967-72

6. Olson AL, Swigris JJ, Lezotte DC, Norris JM, Wilson CG, Brown KK. Mortality from Pulmonary Fibrosis Increased in the United States from 1992 to 2003. Am J Respir Crit Care Med 2007; 176: 277-84

7. Fan LL, Deterding RR, Langston C. Pediatric interstitial lung disease revisited. Pediatric Pulmonology 2004; 38: 369-378

8. Pinheiro GA, Antao VC, Wood JM, Wassell JT. Occupational risks for idiopathic pulmonary fibrosis mortality in the United States. Int J Occup Environ Health 2008; 14: 117-23

9. Newman LS, Mroz MM, Ruttenber AJ. Lung fibrosis in plutonium workers. Radiat Res 2005; 164: 123-31

10. Jules-Elysee K, White DA. Bleomycin-induced pulmonary toxicity. Clin Chest Med 1990; 11: 1-20

11. Agustí C, Xaubet A, Agustí AG, Roca J, Ramirez J, Rodriguez-Roisin R. Clinical and functional assessment of patients with idiopathic pulmonary fibrosis: results of a 3 year follow-up.Eur Respir J 1994; 7: 643-50

12. Cailes JB, O'Connor C, Pantelidis P, Southcott AM, Fitzgerald MX, Black CM, Bois RM. Neutrophil activation in fibrosing alveolitis: a comparison of

lone cryptogenic fibrosing alveolitis and systemic sclerosis. Eur Respir J 1996; 9: 992-999

13. Wells AU, Hansell DM, Rubens MB, Cullinan P, Haslam PL, Black CM, Du Bois RM. Fibrosing alveolitis in systemic sclerosis. Bronchoalveolar lavage findings in relation to computed tomographic appearance. Am J Respir Crit Care Med 1994; 150: 462-8

14. Obayashi Y, Yamadori I, Fujita J, Yoshinouchi T, Ueda N, Takahara J. The role of neutrophils in the pathogenesis of idiopathic pulmonary fibrosis. Chest 1997; 112: 1338-43

15. Losa García JE, Rodríguez FM, Martín de Cabo MR, García Salgado MJ, Losada JP, Villarón LG, López AJ, Arellano JL. Evaluation of inflammatory cytokine secretion by human alveolar macrophages. Mediators Inflamm 1999; 8: 43-51

16. Piguet PF, Ribaux C, Karpuz V, Grau GE, Kapanci Y. Expression and localization of tumor necrosis factor-α and its mRNA in idiopathic pulmonary fibrosis. American Journal of Pathology 1993; 143: 651-655

17. Lesur OJ, Mancini NM, Humbert JC, Chabot F, Polu J-M. Interleukin-6, Interferon-gamma, and phospholipid levels in the alveolar lining fluid of human lungs: profiles in coal worker's pneumoconiosis and idiopathic pulmonary fibrosis. Chest 1994; 106: 407-413

18. Kline JN, Schwartz DA, Monick MM, Floerchinger CS, Hunninghake GW. Relative release of interleukin-1 beta and interleukin-1 receptor antagonist by alveolar macrophages. A study in asbestos-induced lung disease, sarcoidosis, and idiopathic pulmonary fibrosis. Chest 1993; 104: 47-53

19. Jones KP, Reynolds SP, Capper SJ, Kalinka S, Edwards JH, Davies BH. Measurement of interleukin-6 in bronchoalveolar lavage fluid by radioimmunoassay: differences between patients with interstitial lung disease and control subjects. Clin Exp Immunol 1991; 83: 30-4

20. Takizawa H, Satoh M, Okazaki H, Matsuzaki G, Suzuki N, Ishii A, Suko M, Okudaira H, Morita Y, Ito K. Increased IL-6 and IL-8 in bronchoalveolar lavage fluids (BALF) from patients with sarcoidosis: correlation with the clinical parameters. Clin Exp Immunol 1997; 107: 175-81

21. Kapanci Y, Desmouliere A, Pache JC, Redard M, Gabbiani G. Cytoskeletal protein modulation in pulmonary alveolar myofibroblasts during idiopathic pulmonary fibrosis. Possible role of transforming growth factor beta and tumor necrosis factor alpha. Am J Respir Crit Care Med 1995; 152: 2163-9

22. Meltzer EB and Noble PW. Idiopathic pulmonary fibrosis. Orphanet Journal of Rare Diseases 2008, 3: 8

23. Selman M, King TE, Pardo A. Idiopathic pulmonary fibrosis: prevailing and evolving hypotheses about its pathogenesis and implications for therapy. Ann Intern Med 2001; 134: 136-51

24. Selman M, Montaño M, Ramos C, Chapela R. Concentration, biosynthesis and degradation of collagen in idiopathic pulmonary fibrosis. Thorax 1986; 41: 355-9

25. Alberts B, Johnson A, Lewis J, Raff M, Roberts K, Walter P. Molecular biology of the cell. 4th Edition. Garland Science, 2002

26. Stockley RA. Neutrophils and protease/antiprotease imbalance. Am J Respir Crit Care Med 1999; 160: 49-52

27. Chua F, Dunsmore SE, Clingen PH, Mutsaers SE, Shapiro SD, Segal AW, Roes J, Laurent GJ. Mice lacking neutrophil elastase are resistant to bleomycin-induced pulmonary fibrosis. Am J Pathol 2007; 170: 65-74

28. Elias JA, Freundlich B, Kern JA, Rosenbloom J. Cytokine networks in the regulation of inflammation and fibrosis in the lung. Chest 1990; 97: 1439-45

29. Battegay EJ, Raines EW, Colbert T, Ross R. TNF-alpha stimulation of fibroblast proliferation. Dependence on platelet-derived growth factor (PDGF) secretion and alteration of PDGF receptor expression. J Immunol 1995; 154: 6040-7

30. Piguet PF, Vesin C. Treatment by human recombinant soluble TNF receptor of pulmonary fibrosis induced by bleomycin or silica in mice. Eur Respir J 1994; 7: 515-18

31. Denis M. Interleukin-6 in mouse hypersensitivity pneumonitis: changes in lung free cells following depletion of endogenous IL-6 or direct administration of IL-6. J Leukoc Biol 1992; 52: 197-201

32. Yoshida M, Sakuma J, Hayashi S, Abe K, Saito I, Harada S, Sakatani M, Yamamoto S, Matsumoto N, Kaneda Y, et al. A histologically distinctive interstitial pneumonia induced by overexpression of the interleukin 6, transforming growth factor beta 1, or platelet-derived growth factor B gene. Proc Natl Acad Sci U S A 1995; 92: 9570-4

33. Kawanami O, Ferrans VJ, Crystal RG. Structure of alveolar epithelial cells in patients with fibrotic lung disorders. Lab Invest 1982; 46: 39-53

34. Uhal BD, Joshi I, True AL, Mundle S, Raza A, Pardo A, Selman M. Fibroblasts isolated after fibrotic lung injury induce apoptosis of alveolar epithelial cells in vitro. Am J Physiol 1995; 269: 819-28

35. Kotani I, Sato A, Hayakawa H, Urano T, Takada Y, Takada A. Increased procoagulant and antifibrinolytic activities in the lungs with idiopathic pulmonary fibrosis. Thromb Res 1995; 77: 493-504

36. Moodley YP, Caterina P, Scaffidi AK, Misso NL, Papadimitriou JM, McAnulty RJ, Laurent GJ, Thompson PJ, Knight DA. Comparison of the morphological and biochemical changes in normal human lung fibroblasts and fibroblasts derived from lungs of patients with idiopathic pulmonary fibrosis during FasL-induced apoptosis. J Pathol. 2004; 202: 486-95

37. Ramos C, Montaño M, García-Alvarez J, Ruiz V, Uhal BD, Selman M, Pardo A. Fibroblasts from idiopathic pulmonary fibrosis and normal lungs differ in growth rate, apoptosis, and tissue inhibitor of metalloproteinases expression. Am J Respir Cell Mol Biol 2001; 24: 591-8

38. Satomi Y, Tsuchiya W, Miura D, Kasahara Y, Akahori F. DNA microarray analysis of pulmonary fibrosis three months after exposure to paraquat in rats. J Toxicol Sci 2006; 31: 345-55

39. Matsuoka H, Arai T, Mori M, Goya S, Kida H, Morishita H, Fujiwara H, Tachibana I, Osaki T, Hayashi S. A p38 MAPK inhibitor, FR-167653, ameliorates murine bleomycin-induced pulmonary fibrosis. Am J Physiol Lung Cell Mol Physiol 2002; 283: 103-12

40. Shimizu Y, Dobashi K, Iizuka K, Horie T, Suzuki K, Tukagoshi H, Nakazawa T, Nakazato Y, Mori M. Contribution of small GTPase Rho and its target protein rock in a murine model of lung fibrosis. Am J Respir Crit Care Med 2001; 163: 210-7

41. Kuhn C, McDonald JA. The roles of the myofibroblast in idiopathic pulmonary fibrosis. Ultrastructural and immunohistochemical features of sites of active extracellular matrix synthesis. Am J Pathol 1991; 138: 1257-65

42. Suganuma H, Sato A, Tamura R, Chida K. Enhanced migration of fibroblasts derived from lungs with fibrotic lesions. Thorax 1995; 50: 984-9

43. Iwano M, Plieth D, Danoff TM, Xue C, Okada H, Neilson EG. Evidence that fibroblasts derive from epithelium during tissue fibrosis. J Clin Invest 2002; 110: 341-50

44. Kim KK, Kugler MC, Wolters PJ, Robillard L, Galvez MG, Brumwell AN, Sheppard D, Chapman HA. Alveolar epithelial cell mesenchymal transition

develops in vivo during pulmonary fibrosis and is regulated by the extracellular matrix. Proc Natl Acad Sci U S A 2006; 103: 13180-5

45. Andersson-Sjöland A, de Alba CG, Nihlberg K, Becerril C, Ramírez R, Pardo A, Westergren-Thorsson G, Selman M. Fibrocytes are a potential source of lung fibroblasts in idiopathic pulmonary fibrosis. Int J Biochem Cell Biol 2008; 40: 2129-40

46. Lemjabbar H, Gosset P, Lechapt-Zalcman E, Franco-Montoya ML, Wallaert B, Harf A, Lafuma C. Overexpression of alveolar macrophage gelatinase B (MMP-9) in patients with idiopathic pulmonary fibrosis: effects of steroid and immunosuppressive treatment. Am J Respir Cell Mol Biol 1999; 20: 903-13

47. Selman M, Pardo A, Barrera L, Estrada A, Watson SR, Wilson K, Aziz N, Kaminski N, Zlotnik A. Gene expression profiles distinguish idiopathic pulmonary fibrosis from hypersensitivity pneumonitis. Am J Respir Crit Care Med 2006; 173: 188-98

48. Thannickal VJ, Toews GB, White ES, Lynch JP 3rd, Martinez FJ. Mechanisms of pulmonary fibrosis. Annu Rev Med 2004; 55: 395-417

49. Raghu G, Masta S, Meyers D, Narayanan AS. Collagen synthesis by normal and fibrotic human lung fibroblasts and the effect of transforming growth factor-beta. Am Rev Respir Dis 1989; 140: 95-100

50. Chapman HA. Disorders of lung matrix remodeling. J Clin Invest 2004; 113: 148-57

51. Moeller A, Ask K, Warburton D, Gauldie J, Kolb M. The bleomycin animal model: a useful tool to investigate treatment options for idiopathic pulmonary fibrosis? Int J Biochem Cell Biol 2008; 40: 362-82

52. Fleischmann RW, Baber JR, Thompson GR, Schaeppi UH, Illievsky VR, Cooney DA, Davis RD. Bleomycin-induced interstitial pneumonia in dogs. Thorax 1971; 26 :675-82

53. Adamson IY, Bowden DH. The pathogenesis of bleomycin-induced pulmonary fibrosis in mice. Am J Pathol 1974; 77: 185-97

54. Chua F, Gauldie J, Laurent GJ. Pulmonary fibrosis: searching for model answers. Am J Respir Cell Mol Biol 2005; 33: 9-13

55. Lasky JA, Ortiz L. Bleomycin-induced lung injury. www.uptodate.com/patients. Last time updated: October 9, 2008. Last time accessed: December 19, 2008

56. Sikic BI. Biochemical and cellular determinants of bleomycin cytotoxicity. Cancer Surv 1986; 5: 81-91

57. Lazo JS, Merrill WW, Pham ET, Lynch TJ, McCallister JD, Ingbar DH. Bleomycin hydrolase activity in pulmonary cells. J Pharmacol Exp Ther 1984; 231: 583-8

58. Chandler DB. Possible mechanisms of bleomycin-induced fibrosis. Clin Chest Med 1990; 11: 21-30

59. Murakami S, Nagaya N, Itoh T, Kataoka M, Iwase T, Horio T, Miyahara Y, Sakai Y, Kangawa K, Kimura H. Prostacyclin agonist with thromboxane synthase inhibitory activity (ONO-1301) attenuates bleomycin-induced pulmonary fibrosis in mice. Am J Physiol Lung Cell Mol Physiol 2006; 290: 59-65

60. Nagano J, Iyonaga K, Kawamura K, Yamashita A, Ichiyasu H, Okamoto T, Suga M, Sasaki Y, Kohrogi H. Use of tacrolimus, a potent antifibrotic agent, in bleomycin-induced lung fibrosis. Eur Respir J 2006; 27: 460-9

61. Keogh KA, Standing J, Kane GC, Terzic A, Limper AH. Angiotensin II antagonism fails to ameliorate bleomycin-induced pulmonary fibrosis in mice. Eur Respir J 2005; 25: 708-14

62. Chaudhary NI, Schnapp A, Park JE. Pharmacologic differentiation of inflammation and fibrosis in the rat bleomycin model. Am J Respir Crit Care Med 2006; 173: 769-76

63. Aono Y, Nishioka Y, Inayama M, Ugai M, Kishi J, Uehara H, Izumi K, Sone S. Imatinib as a novel antifibrotic agent in bleomycin-induced pulmonary fibrosis in mice. Am J Respir Crit Care Med 2005; 171: 1279-85

64. Saito F, Tasaka S, Inoue K, Miyamoto K, Nakano Y, Ogawa Y, Yamada W, Shiraishi Y, Hasegawa N, Fujishima S, Takano H, Ishizaka A. Role of interleukin-6 in bleomycin-induced lung inflammatory changes in mice. Am J Respir Cell Mol Biol 2008; 38: 566-71

65. Izbicki G, Segel MJ, Christensen TG, Conner MW, Breuer R. Time course of bleomycin-induced lung fibrosis. Int J Exp Path 2002; 83: 111-119

66. Gharaee-Kermani M, Hatano K, Nozaki Y, Phan SH. Gender-based differences in bleomycin-induced pulmonary fibrosis. Am J Pathol 2005; 166: 1593-606

67. Schwartz DA, Helmers RA, Galvin JR, Van Fossen DS, Frees KL, Dayton CS, Burmeister LF, Hunninghake GW. Determinants of survival in idiopathic pulmonary fibrosis. Am J Respir Crit Care Med 1994; 149: 450-4

68. Panos RJ, Mortenson RL, Niccoli SA, King TE Jr. Clinical deterioration in patients with idiopathic pulmonary fibrosis: causes and assessment. Am J Med 1990; 88: 396-404

69. Selman M, Carrillo G, Estrada A, Mejia M, Becerril C, Cisneros J, Gaxiola M, Pérez-Padilla R, Navarro C, Richards T, Dauber J, King TE Jr, Pardo A, Kaminski N. Accelerated variant of idiopathic pulmonary fibrosis: clinical behavior and gene expression pattern. PLoS ONE 2007; 2: e482

70. Hubbard R, Venn A, Lewis S, Britton J. Lung cancer and cryptogenic fibrosing alveolitis. A population-based cohort study. Am J Respir Crit Care Med 2000; 161: 5-8

71. Wells C, Mannino DM. Pulmonary fibrosis and lung cancer in the United States: analysis of the multiple cause of death mortality data, 1979 through 1991. South Med J 1996; 89: 505-10

72. Fiorucci E, Lucantoni G, Paone G, Zotti M, Li BE, Serpilli M, Regimenti P, Cammarella I, Puglisi G, Schmid G. Colchicine, cyclophosphamide and prednisone in the treatment of mild-moderate idiopathic pulmonary fibrosis: comparison of three currently available therapeutic regimens. Eur Rev Med Pharmacol Sci 2008; 12: 105-11

73. American Hospital Formulary Service® (AHFS™) drug information. American Society of Health-System Pharmacists (ASHP). www.ashp.org/mngrphs/ahfs/. Last edition: 2009.Last accessed: December 19, 2008

74. Raghu G, Johnson WC, Lockhart D, Mageto Y. Treatment of idiopathic pulmonary fibrosis with a new antifibrotic agent, pirfenidone: results of a prospective, open-label Phase II study. Am J Respir Crit Care Med 1999; 159: 1061-9

75. Ziesche R, Hofbauer E, Wittmann K, Petkov V, Block LH. A preliminary study of long-term treatment with interferon gamma-1b and low-dose prednisolone in patients with idiopathic pulmonary fibrosis. N Engl J Med 1999; 341: 1264-9

76. Behr J, Maier K, Degenkolb B, Krombach F, Vogelmeier C. Antioxidative and clinical effects of high-dose N-acetylcysteine in fibrosing alveolitis. Adjunctive therapy to maintenance immunosuppression. Am J Respir Crit Care Med 1997; 156: 1897-901

77. Giri SN, Hyde DM, Hollinger MA. Effect of antibody to transforming growth factor beta on bleomycin induced accumulation of lung collagen in mice. Thorax 1993; 48: 959-66

78. Hagiwara S, Iwasaka H, Matsumoto S, Noguchi T. Introduction of antisense oligonucleotides to heat shock protein 47 prevents pulmonary fibrosis in lipopolysaccharide-induced pneumopathy of the rat. Eur J Pharmacol 2007; 564: 174-80

79. Serrano-Mollar A, Nacher M, Gay-Jordi G, Closa D, Xaubet A, Bulbena O. Intratracheal transplantation of alveolar type II cells reverses bleomycin-induced lung fibrosis. Am J Respir Crit Care Med 2007; 176: 1261-8

80. Ortiz LA, Gambelli F, McBride C, Gaupp D, Baddoo M, Kaminski N, Phinney DG. Mesenchymal stem cell engraftment in lung is enhanced in response to bleomycin exposure and ameliorates in fibrotic effects. Proc Natl Acad Sci U S A 2003; 100: 8407-11

81. Rojas M, Xu J, Woods CR, Mora AL, Spears W, Roman J, Brigham KL. Bone marrow-derived mesenchymal stem cells in repair of the injured lung. Am. J. Respir. Am J Respir Cell Mol Biol 2005; 33: 145-52

82. Ghofrani HA, Wiedemann R, Rose F, Schermuly RT, Olschewski H, Weissmann N, Gunther A, Walmrath D, Seeger W, Grimminger F. Sildenafil for treatment of lung fibrosis and pulmonary hypertension: a randomised controlled trial. Lancet 2002; 360: 895-900

83. Trulock EP, Christie JD, Edwards LB, Boucek MM, Aurora P, Taylor DO, Dobbels F, Rahmel AO, Keck BM, Hertz MI. Registry of the International Society for Heart and Lung Transplantation: twenty-fourth official adult lung and heart-lung transplantation report-2007. J Heart Lung Transplant 2007; 26: 782-95

84. Bender AT, Beavo JA. Cyclic nucleotide phosphodiesterases: molecular regulation to clinical use. Pharmacol Rev 2006; 58: 488-520

85. Conti M, Beavo J. Biochemistry and physiology of cyclic nucleotide phosphodiesterases: essential components in cyclic nucleotide signaling. Annu Rev Biochem 2007;76: 481-511

86. Lugnier C. Cyclic nucleotide phosphodiesterase (PDE) superfamily: a new target for the development of specific therapeutic agents. Pharmacol Ther 2006; 109: 366-98

87. Omori K, Kotera J. Overview of PDEs and their regulation. Circ Res 2007; 100: 309-27

88. Expert Protein Analysis System (EXPASY) proteomics server. Swiss Institute of Bioinformatics. http://www.expasy.org/enzyme/3.1.4.17. Last time accessed: December 19, 2008

89. Obernolte R, Bhakta S, Alvarez R, Bach C, Zuppan P, Mulkins M, Jarnagin K, Shelton ER. The cDNA of a human lymphocyte cyclic-AMP phosphodiesterase (PDE IV) reveals a multigene family. Gene 1993; 129: 239-47

90. J Richter W, Conti M. The oligomerization state determines regulatory properties and inhibitor sensitivity of type 4 cAMP-specific phosphodiesterases. Biol Chem. 2004 Jul 16;279(29):30338-48. Epub 2004 May 6.

91. Card GL, England BP, Suzuki Y, Fong D, Powell B, Lee B, Luu C, Tabrizizad M, Gillette S, Ibrahim PN, Artis DR, Bollag G, Milburn MV, Kim SH, Schlessinger J, Zhang KY. Structural basis for the activity of drugs that inhibit phosphodiesterases. Structure 2004; 12: 2233-47

92. McLaughlin MM, Cieslinski LB, Burman M, Torphy TJ, Livi GP. A low-Km, rolipram-sensitive, cAMP-specific phosphodiesterase from human brain. Cloning and expression of cDNA, biochemical characterization of recombinant protein, and tissue distribution of mRNA. J Biol Chem 1993; 268: 6470-6

93. Engels P, Fichtel K, Lübbert H. Expression and regulation of human and rat phosphodiesterase type IV isogenes. FEBS Lett 1994; 350: 291-5

94. Engels P, Sullivan M, Muller T, Lubbert H. Molecular cloning and functional expression in yeast of a human cAMP-specific phosphodiesterase subtype (PDE IV-C). FEBS Lett 1995; 358: 305-10

95. Wang P, Wu P, Ohleth KM, Egan RW, Billah MM. Phosphodiesterase 4B2 is the predominant phosphodiesterase species and undergoes differential regulation of gene expression in human monocytes and neutrophils. Mol Pharmacol1999; 56: 170-174

96. Shepherd M, McSorley T, Olsen AE, Johnston LA, Thomson NC, Baillie GS, Houslay MD, Bolger GB. Molecular cloning and subcellular distribution of the novel PDE4B4 cAMP-specific phosphodiesterase isoform. Biochem J 2003; 370: 429-38

97. Obernolte R, Ratzliff J, Baecker PA, Daniels DV, Zuppan P, Jarnagin K, Shelton ER. Multiple splice variants of phosphodiesterase PDE4C cloned from human lung and testis. Biochim Biophys Acta 1997; 1353: 287-97

98. Martin-Chouly CA, Astier A, Jacob C, Pruniaux MP, Bertrand C, Lagente V. Modulation of matrix metalloproteinase production from human lung fibroblasts by type 4 phosphodiesterase inhibitors. Life Sci 2004; 75: 823-40

99. Barnes AP, Livera G, Huang P, Sun C, O'Neal WK, Conti M, Stutts MJ, Milgram SL. Phosphodiesterase 4D forms a cAMP diffusion barrier at the apical membrane of the airway epithelium. J Biol Chem 2005; 280: 7997-8003

100. Livi GP, Kmetz P, McHale MM, Cieslinski LB, Sathe GM, Taylor DP, Davis RL, Torphy TJ, Balcarek JM. Cloning and expression of cDNA for a human low-Km, rolipram-sensitive cyclic AMP phosphodiesterase. Mol Cell Biol 1990; 10: 2678-86

101. Souness JE, Griffin M, Maslen C, Ebsworth K, Scott LC, Pollock K, Palfreyman MN, Karlsson JA. Evidence that cyclic AMP phosphodiesterase inhibitors suppress TNF alpha generation from human monocytes by interacting with a 'low-affinity' phosphodiesterase 4 conformer. Br J Pharmacol 1996; 118: 649-58

102. Erdogan S, Houslay MD. Challenge of human Jurkat T-cells with the adenylate cyclase activator forskolin elicits major changes in cAMP phosphodiesterase (PDE) expression by up-regulating PDE3 and inducing PDE4D1 and PDE4D2 splice variants as well as down-regulating a novel PDE4A splice variant. Biochem J 1997; 321: 165-75

103. Zhang X, Odom DT, Koo SH, Conkright MD, Canettieri G, Best J, Chen H, Jenner R, Herbolsheimer E, Jacobsen E, Kadam S, Ecker JR, Emerson B, Hogenesch JB, Unterman T, Young RA, Montminy M. Genome-wide analysis of cAMP-response element binding protein occupancy, phosphorylation, and target gene activation in human tissues. Proc Natl Acad Sci U S A 2005; 102: 4459-64

104. Jin SL, Conti M. Induction of the cyclic nucleotide phosphodiesterase PDE4B is essential for LPS-activated TNF-alpha responses. Proc Natl Acad Sci U S A 2002; 99: 7628-33

105. Jin SL, Lan L, Zoudilova M, Conti M. Specific role of phosphodiesterase 4B in lipopolysaccharide-induced signaling in mouse macrophages. J Immunol 2005; 175: 1523-31

106. Clark JG, Kostal KM, Marino BA. Bleomycin-induced pulmonary fibrosis in hamsters. An alveolar macrophage product increases fibroblast prostaglandin E2 and cyclic adenosine monophosphate and suppresses fibroblast proliferation and collagen production. J Clin Invest 1983; 72: 2082-91

107. Kohyama T, Liu X, Kim HJ, Kobayashi T, Ertl RF, Wen FQ, Takizawa H, Rennard SI. Prostacyclin analogs inhibit fibroblast migration. Am J Physiol Lung Cell Mol Physiol 2002; 283: L428-32

108. Kohyama T, Liu XD, Wen FQ, Kim HJ, Takizawa H, Rennard SI. Prostaglandin D2 inhibits fibroblast migration. Eur Respir J 2002; 19: 684-9

109. Kolodsick JE, Peters-Golden M, Larios J, Toews GB, Thannickal VJ, Moore BB. Prostaglandin E2 inhibits fibroblast to myofibroblast transition via E prostanoid 2 signaling and cyclic adenosine monophosphate elevation. Am J Respir Cell Mol Biol 2003; 29: 537-44

110. Dunkern TR, Feurstein D, Rossi GA, Sabatini F, Hatzelmann A. Inhibition of TGF-beta induced lung fibroblast to myofibroblast conversion by phosphodiesterase inhibiting drugs and activators of soluble guanylyl cyclase. Eur J Pharmacol 2007; 572: 12-22

111. Dumaz N, Marais R. Integrating signals between cAMP and the RAS/RAF/MEK/ERK signalling pathways. FEBS Journal 2005; 272: 3491-3504

112. Alvarez R, Sette C, Yang D, Eglen RM, Wilhelm R, Shelton ER, Conti M. Activation and selective inhibition of a cyclic AMP-specific phosphodiesterase, PDE-4D3. Mol Pharmacol 1995; 48: 616-22

113. Sette C, Conti M. Phosphorylation and activation of a cAMP-specific phosphodiesterase by the cAMP-dependent protein kinase. Involvement of serine 54 in the enzyme activation. J Biol Chem 1996; 271: 16526-34

114. Jin SL, Bushnik T, Lan L, Conti M. Subcellular localization of rolipram-sensitive, cAMP-specific phosphodiesterases. Differential targeting and activation of the splicing variants derived from the PDE4D gene. J Biol Chem 1998; 273: 19672-8

115. Lynch MJ, Baillie GS, Mohamed A, Li X, Maisonneuve C, Klussmann E, van Heeke G, Houslay MD. RNA silencing identifies PDE4D5 as the functionally relevant cAMP phosphodiesterase interacting with beta arrestin to control the protein kinase A/AKAP79-mediated switching of the beta2-adrenergic receptor to activation of ERK in HEK293B2 cells. J Biol Chem 2005; 280: 33178-89

116. Houslay MD, Adams DR. PDE4 cAMP phosphodiesterases: modular enzymes that orchestrate signalling cross-talk, desensitization and compartmentalization. Biochem J 2003; 370: 1-18

117. Vicini E, Conti M. Characterization of an intronic promoter of a cyclic adenosine 3',5'-monophosphate (cAMP)-specific phosphodiesterase gene that confers hormone and cAMP inducibility. Mol Endocrinol 1997; 11: 839-50

118. Ma D, Wu P, Egan RW, Billah MM, Wang P. Phosphodiesterase 4B gene transcription is activated by lipopolysaccharide and inhibited by interleukin-10 in human monocytes. Mol Pharmacol 1999; 55: 50-7

119. Manning CD, Burman M, Christensen SB, Cieslinski LB, Essayan DM, Grous M, Torphy TJ, Barnette MS. Suppression of human inflammatory cell function by subtype-selective PDE4 inhibitors correlates with inhibition of PDE4A and PDE4B. Br J Pharmacol 1999; 128: 1393-8

120. Abrahamsen H, Baillie G, Ngai J, Vang T, Nika K, Ruppelt A, Mustelin T, Zaccolo M, Houslay M, Tasken K. TCR- and CD28-mediated recruitment of phosphodiesterase 4 to lipid rafts potentiates TCR signaling. J Immunol 2004; 173: 4847-58

121. Ariga M, Neitzert B, Nakae S, Mottin G, Bertrand C, Pruniaux MP, Jin SL, Conti M. Nonredundant function of phosphodiesterases 4D and 4B in neutrophil recruitment to the site of inflammation. J Immunol 2004; 173: 7531-8

122. Rivedal E, Sanner T. Caffeine and other phosphodiesterase inhibitors are potent inhibitors of the promotional effect of TPA on morphological transformation of hamster embryo cells. Cancer Lett 1985; 28: 9-17

123. Schwabe U, Miyake M, Ohga Y, Daly JW. 4-(3-Cyclopentyloxy-4-methoxyphenyl)-2-pyrrolidone (ZK 62711): a potent inhibitor of adenosine cyclic 3',5'-monophosphate phosphodiesterases in homogenates and tissue slices from rat brain. Mol Pharmacol 1976; 12: 900-10

124. Torphy TJ, Undem BJ. Phosphodiesterase inhibitors: new opportunities for the treatment of asthma. Thorax 1991; 46: 512-23

125. Lagente V, Moodley I, Perrin S, Mottin G, Junien JL. Effects of isozyme-selective phosphodiesterase inhibitors on eosinophil infiltration in the guinea-pig lung. Eur J Pharmacol 1994; 255: 253-6

126. Robichaud A, Stamatiou PB, Jin SL, Lachance N, MacDonald D, Laliberte F, Liu S, Huang Z, Conti M, Chan CC. Deletion of phosphodiesterase 4D in

mice shortens alpha (2)-adrenoceptor-mediated anesthesia, a behavioral correlate of emesis. J Clin Invest 2002; 110: 1045-52

127. Christensen SB, Guider A, Forster CJ, Gleason JG, Bender PE, Karpinski JM, DeWolf WE Jr, Barnette MS, Underwood DC, Griswold DE, Cieslinski LB, Burman M, Bochnowicz S, Osborn RR, Manning CD, Grous M, Hillegas LM, Bartus JO, Ryan MD, Eggleston DS, Haltiwanger RC, Torphy TJ. 1,4-Cyclohexanecarboxylates: potent and selective inhibitors of phosophodiesterase 4 for the treatment of asthma. J Med Chem 1998; 41: 821-35

128. Zussman BD, Benincosa LJ, Webber DM, Clark DJ, Cowley H, Kelly J, Murdoch RD, Upward J, Wyld P, Port A, Fuder H. An overview of the pharmacokinetics of cilomilast (Ariflo), a new, orally active phosphodiesterase 4 inhibitor, in healthy young and elderly volunteers. J Clin Pharmacol 2001; 41: 950-8

129. Zussman BD, Davie CC, Kelly J, Murdoch RD, Clark DJ, Schofield JP, Walls C, Birrell C, Webber D, Quinlan J, Ritchie SY, Carr A. Bioavailability of the oral selective phosphodiesterase 4 inhibitor cilomilast. Pharmacotherapy 2001; 21: 653-60

130. Down G, Siederer S, Lim S, Daley-Yates P. Clinical pharmacology of Cilomilast. Clin Pharmacokinet 2006; 45: 217-33.

131. Drug Development Technology. Ariflo (Cilomilast) - Oral PDE-IV Inhibitor for Chronic Obstructive Pulmonary Disease (COPD). http://www.drugdevelopment-technology.com/projects/ariflo/. Last time accessed: December 23, 2008

132. Lagente V, Martin-Chouly C, Boichot E, Martins MA, Silva PM. Selective PDE4 inhibitors as potent anti-inflammatory drugs for the treatment of airway diseases. Mem Inst Oswaldo Cruz 2005; 1: 131-6

133. Giri SN, Sanford DA Jr, Robison TW, Tyler NK. Impairment in coupled beta-adrenergic receptor and adenylate cyclase system during bleomycin-induced lung fibrosis in hamsters. Exp Lung Res 1987; 13: 401-16

134. Griswold DE, Webb EF, Badger AM, Gorycki PD, Levandoski PA, Barnette MA, Grous M, Christensen S, Torphy TJ. SB 207499 (Ariflo), a second generation phosphodiesterase 4 inhibitor, reduces tumor necrosis factor α and interleukin-4 production in vivo. J Pharmacol Exp Ther 1998; 287: 705-11

135. Corbel M, Germain N, Lanchou J, Molet S, Silva PM, Martins MA, Boichot E, Lagente V. The selective phosphodiesterase 4 inhibitor PR 73-401 reduced matrix metalloproteinase 9 activity and transforming growth factor-β release

during acute lung injury in mice: the role of the balance between tumor necrosis factor-α and interleukin-10. J Pharmacol Exp Ther 2002; 301: 258-65

136. Wollin L, Bundschuh DS, Wohlsen A, Marx D, Beume R. Inhibition of airway hyperresponsiveness and pulmonary inflammation by roflumilast and other PDE4 inhibitors. Pulm Pharmacol Ther 2006; 19: 343-52

137. Ouagued M, Martin-Chouly CA, Brinchault G, Leportier-Comoy C, Depincé A, Bertrand C, Lagente V, Belleguic C, Pruniaux MP. The novel phosphodiesterase 4 inhibitor, CI-1044, inhibits LPS-induced TNF-alpha production in whole blood from COPD patients. Pulm Pharmacol Ther 2005; 18: 49-54

138. Videla S, Vilaseca J, Medina C, Mourelle M, Guarner F, Salas A, Malagelada J-R. Selective inhibition of phosphodiesterase-4 ameliorates chronic colitis and prevents intestinal fibrosis. J Pharmacol Exp Ther 2006; 316: 940-5

139. Liu X, Rennolds SO, Paul AI. cAMP elevating agents and adenylyl cyclase overexpression promote an antifibrotic phenotype in pulmonary fibroblasts. Am J Physiol Cell Physiol 2004; 286: C1089-99

140. Wilborn J, Crofford LJ, Burdick MD, Kunkel SL, Strieter RM, Peters-Golden M. Cultured lung fibroblasts isolated from patients with idiopathic pulmonary fibrosis have a diminished capacity to synthesize prostaglandin E2 and to express cyclooxygenase-2. J Clin Invest 1995; 95: 1861-8

141. Dubey RK, Gillespie DG, Mi Z, Jackson EK. Endogenous cyclic AMP-adenosine pathway regulates cardiac fibroblast growth. Hypertension 2001; 37: 1095-1100

142. Growcott EJ, Spink KG, Ren X, Afzal S, Banner KH, Wharton J. Phosphodiesterase type 4 expression and anti-proliferative effects in human pulmonary artery smooth muscle cells. Respir Res 2006; 7: 9

143. Kohyama T, Liu X, Zhu YK, Wen F-Q, Wang HJ, Fang Q, Kobayashi T, Rennard SI. Phosphodiesterase 4 inhibitor cilomilast inhibits fibroblast-mediated collagen gel degradation induced by tumor necrosis factor-α and neutrophil elastase. Am J Respir Cell Mol Biol 2002; 27: 487-94

144. Pullamsetti S, Krick S, Yilmaz H, Ghofrani HA, Schudt C, Weissmann N, Fuchs B, Seeger W, Grimminger F, Schermuly RT. Inhaled tolafentrine reverses pulmonary vascular remodeling via inhibition of smooth muscle cell migration. Respir Res 2005; 6:128

145. Ashcroft T, Simpson JM, Timbrell V. Simple method of estimating severity of pulmonary fibrosis on a numerical scale. J Clin Pathol 1988; 41: 467-70

146. Prabhakar U, Lipshutz D, Bartus JO, Slivjak MJ, Smith EF 3rd, Lee JC, Esser KM. Characterization of cAMP-dependent inhibition of LPS-induced TNF alpha production by rolipram, a specific phosphodiesterase IV (PDE IV) inhibitor. Int J Immunopharmacol 1994; 16: 805-16

147. Zhang HY, Gharaee-Kermani M, Phan SH. Regulation of lung fibroblast alpha-smooth muscle actin expression, contractile phenotype, and apoptosis by IL-1beta. J Immunol 1997; 158: 1392-9

7. Declaration

I declare that I have completed this dissertation single-handedly without the unauthorized help of a second party and only with the assistance acknowledged therein. I have appropriately acknowledged and referenced all text passages that are derived literally from or are based on the content of published or unpublished work of others, and all information that relates to verbal communications. I have abided by the principles of good scientific conduct laid down in the charter of the Justus Liebig University of Giessen in carrying out the investigations described in the dissertation.

8. Acknowledgements

At the end of this work I would like to sincerely thank the people that directly or indirectly made this project possible and helped me to gain the cutting-edge scientific experience.

First of all, I would like to express my gratitude to my supervisor Prof. Dr. Ralph Theo Schermuly as this novel project would, obviously, not exist without his guidance. I thank him for his ability to organize the working process and everything what could be necessary for it as this is so much important in every scientific effort. I would also like to thank you for healthy criticism, for sharing with me your scientific experience and for the productive advises in the situations when I needed them!

I would also like to deeply thank our postdocs, Dr. Soni Savai-Pullamsetti and, particularly, Dr. Rio Dumitrascu who was simply my teacher in the day-to-day animal experimental work. Thank you both so much for the priceless suggestions, criticism and support!

Similarly, I would like to acknowledge our technicians and the lab staff of Dr. Norbert Weissmann and Dr. Hossein Ardeschir Ghofrani for expending our experimental facilities; I would also like to thank the lab of Prof. Dr. Jürgen Lohmeyer for providing the facilities for the differential BALF cell count. We also thank Nycomed Europe GmbH for providing cilomilast.

Separately, I thank the organizers and the faculty of MBML graduate program, in particular, Dr. Werner Seeger, Dr. Friedrich Grimminger, Dr. Oliver Eickelberg and Dr. Rory Morty for giving me the opportunity to immerse into the intense but very effective learning process and to gain the new scientific knowledge.

Needless to mention, day-to-day communication and the spirit in the lab are everything. It was a true pleasure to work with the people that created friendly and productive atmosphere. I address my sincere acknowledgements to all the people of our physiology division and especially to Eva Dony, Silke Koebrich and Anke Voigt for sharing with me their experience and emotional involvement! Equally, I am grateful to all the people in our molecular biology division and especially to Piotr Sklepkiewicz, Ewa Kolosionek, Xia Tian, Dr. Kathrin Woyda and Dr. Ying-Ju Lai for their openness and productive discussions!